




## Article

# Decoupling Analysis of Ignition Processes of Ammonia/N-Heptane Mixtures

Zheng Li <sup>1</sup>, Yilin Zhang <sup>1</sup>, Jingrui Li <sup>1,2,3,\*</sup>, Changchun Xu <sup>1,2,3</sup>, Huabing Wen <sup>1</sup>, Jianhua Shen <sup>3</sup>, Haiguo Jing <sup>3</sup>, Haifeng Liu <sup>4</sup>, Xinyan Wang <sup>5</sup> and Hua Zhao <sup>5</sup>

<sup>1</sup> School of Energy and Power, Jiangsu University of Science and Technology, Zhenjiang 212003, China; 222241808413@stu.just.edu.cn (Z.L.); 222241808335@stu.just.cn (Y.Z.); xccgh78006@just.edu.cn (C.X.); whb@just.edu.cn (H.W.)

<sup>2</sup> School of Ship and Ocean Engineering, Jiangsu University of Science and Technology, Zhenjiang 212003, China

<sup>3</sup> CSSC Marine Power Zhenjiang Co., Ltd., Zhenjiang 212001, China; sjh@cssc-cmp.cn (J.S.); jinghaiguo@cssc-cmp.cn (H.J.)

<sup>4</sup> State Key Laboratory of Engine, Tianjin University, Tianjin 300350, China; haifengliu@tju.edu.cn

<sup>5</sup> Center for Advanced Powertrain and Fuels, Brunel University London, London UB8 3PH, UK; xinyan.wang@brunel.ac.uk (X.W.); hua.zhao@brunel.ac.uk (H.Z.)

\* Correspondence: lijingrui@just.edu.cn

**Abstract:** To further understand the influence of n-heptane on the ignition process of ammonia, an isotope labeling method was applied in the current investigation to decouple the influence of the chemical effect, the thermal effect, and the effect of O radical from the oxidation of n-heptane on the ignition delay times (IDTs) of ammonia. An analysis of the time evolution of fuel, analysis of the time evolution of temperature, rate of consumption and production (ROP) analysis, and sensitivity analysis were conducted to gain a further understanding of the mechanism of the influence of the chemical effect, the thermal effect, and the effect of O radical on the ignition of ammonia. The results showed that the negative temperature coefficient (NTC) behavior of n-heptane is mitigated by the blending of ammonia, and this mitigated effect of ammonia is mainly due to the chemical effect. The IDTs of ammonia under low and medium temperatures are significantly shortened by the chemical effect at a n-heptane mass fraction of 10%. The promoting effect of the chemical effect decreases when the n-heptane mass fraction increases. The time evolution of n-heptane for NC<sub>7</sub>H<sub>16</sub>/ND<sub>3</sub>-G can be classified into three stages at 800 K, and the rapid consumption stage is mitigated by an increase in temperature. The rapid consumption stage is suppressed by the chemical effect of ammonia, while O radical has a promoting effect on the rapid consumption stage. The chemical effect will enhance the sensitivities of reactions associated with ammonia. As the n-heptane mass fraction increases, the sensitivities of reactions associated with n-heptane are enhanced. Correspondingly, the effect of reactions associated with ammonia is weakened. When the n-heptane mass fraction is 30%, only reactions related to n-heptane have a great influence on the ignition of ammonia/n-heptane fuel blends under the thermal effect + the effect of O radical or only the thermal effect.

**Keywords:** ignition delay time; chemical effect; thermal effect; ammonia/n-heptane mixtures



**Citation:** Li, Z.; Zhang, Y.; Li, J.; Xu, C.; Wen, H.; Shen, J.; Jing, H.; Liu, H.; Wang, X.; Zhao, H. Decoupling Analysis of Ignition Processes of Ammonia/N-Heptane Mixtures. *Energies* **2024**, *17*, 4938. <https://doi.org/10.3390/en17194938>

Academic Editors: Jamie W.G. Turner and Pavel A. Strizhak

Received: 27 August 2024

Revised: 25 September 2024

Accepted: 30 September 2024

Published: 2 October 2024



**Copyright:** © 2024 by the authors. Licensee MDPI, Basel, Switzerland. This article is an open access article distributed under the terms and conditions of the Creative Commons Attribution (CC BY) license (<https://creativecommons.org/licenses/by/4.0/>).

## 1. Introduction

With the increasing frequency of extreme weather events around the world, global warming has become a big concern [1–4]. CO<sub>2</sub> is the main greenhouse gas and the primary cause of global warming, and mainly comes from the combustion of fossil fuels [5,6]. Therefore, many countries have taken strict measures to reduce carbon emissions. One of the main sources of carbon emissions is the transportation industry. In this sense, the study of carbon-free or renewable alternative fuels has drawn more and more attention. Ammonia is regarded as one of the ideal green fuels owing to the following outstanding properties: (a)

carbon-free; (b) easy to store and transport; and (c) synthesized by fossil fuels or renewable energy [7–10]. Moreover, ammonia also has excellent anti-knock performance when used in internal combustion engines [11,12]. However, engines fueled with ammonia suffer from the ultra-high ignition temperature and extremely slow flame speed of ammonia [9,13].

Due to the excellent anti-knock performance of ammonia, spark ignition ammonia engines have been widely investigated [7,9,10,14,15]. However, whether of pure ammonia or ammonia mixed fuels are utilized, the combustion and thermal efficiency of spark ignition engines is not satisfactory owing to the low flame-propagation velocity of ammonia [11,16,17]. The compression ignition of ammonia does not suffer from the low flame-propagation velocity of ammonia. Nonetheless, the direct utilization of pure ammonia in compression ignition engines has also been proven unsuccessful with a compression ratio that is under 35 due to the high ignition temperature required [18]. At an ultra-high compression ratio, the mechanical load is too high, resulting in a reduced service life of engines. Existing research has found that adding a small amount of high-activity fuels is one of most promising measures for the utilization of ammonia in internal combustion engines [19–21]. Diesel is the most common high-activity fuel, which can be used to shorten the IDTs of ammonia. However, when considering the injection of diesel to shorten the IDTs of ammonia, attention must be paid to the compatibility of mixtures and the impact of the low activity of ammonia on the ignition chemistry [22]. Therefore, in-depth understanding of the interaction mechanism during the ignition process of mixtures is important for the ignition and combustion control of engines. The promoting effects of diesel on the ignition of ammonia can be divided into the chemical and the thermal effect. The chemical effect refers to the influence of intermediate productions generated from the oxidation of diesel, whereas the thermal effect refers to the increasing temperature caused by heat release from the oxidation of diesel. Decoupling the effects of the thermal effect and the chemical effect of diesel on the ignition of ammonia is conducive to controlling the ignition process of ammonia/diesel mixtures. Therefore, the aim of the current study is to reveal the influence of the thermal effect and the chemical effect of diesel on the ignition of ammonia, which is beneficial for controlling the ignition process and improving the thermal efficiency of ammonia/diesel dual-fuel engines.

Diesel is composed of hundreds or thousands of compositions, including alkanes, cycloalkanes, aromatics, etc. [23]. The compositions of diesel are also influenced by the source and production process. It is impossible to directly study the ignition delay time (IDT) of diesel. Owing to its closed IDTs, *n*-heptane is primarily used as a surrogate fuel of diesel [24,25]. The ignition characteristics of  $\text{NC}_7\text{H}_{16}$  have been extensively studied, and its negative temperature coefficient (NTC) behavior has been observed. When the proportion of diesel exceeds a certain value, the NTC behavior also exists in the ignition processes of  $\text{NH}_3/\text{NC}_7\text{H}_{16}$  mixtures. However, in depth understanding of the thermal effect and the chemical effect of *n*-heptane on the IDTs of ammonia in the NTC region need to be further explored.

Scholars have performed extensive studies on the ignition, combustion, and emissions of ammonia/diesel dual-fuel engines. However, these studies have limited insights into the ignition mechanism of ammonia/diesel mixtures. Especially, the influence of the thermal effect and the chemical effect of the ignition of diesel on the IDTs of ammonia are rarely reported. Numerous investigations have been conducted to study the IDTs of ammonia/diesel fuel blends based on single cylinder engines, shock tubes (STs), rapid compression machines (RCMs), and Ansys Chemkin 18.0 software. An experimental study was conducted by Yu et al. [26] to investigate the IDTs of five  $\text{NH}_3/\text{NC}_7\text{H}_{16}$  mixtures with ammonia energy fractions of 0%, 20%, 40%, 60%, and 80% in an RCM. The results showed that the ammonia energy fraction increasing resulted in an increase in the first stage and total IDTs of  $\text{NH}_3/\text{NC}_7\text{H}_{16}$  mixtures. Then, the study developed an ammonia/*n*-heptane dual-fuel mechanism. This dual-fuel mechanism can reproduce the inhibiting effect of the addition of  $\text{NH}_3$  on the IDTs of  $\text{NC}_7\text{H}_{16}$ . Furthermore, the trend of IDTs when the oxygen concentration and equivalence ratio are changed can also be

predicted by the dual-fuel mechanism. However, the predicted IDTs of  $\text{NH}_3/\text{NC}_7\text{H}_{16}$  mixtures by this mechanism are only close to experimental data under controlled conditions. Feng et al. [26] investigated the ignition properties of ammonia-diesel binary fuels with various ammonia blending ratios in an RCM. They studied the NTC behavior and two-stage ignition for the different blends. The first-stage IDTs and total IDTs of ammonia-diesel mixtures increase with an increase in the ammonia energy ratio, and the IDT versus ammonia energy ratio is non-linear. They merged the existing diesel and ammonia mechanisms into a new dual-fuel mechanism. The inhibitory effect of the ammonia blending ratio on the IDTs of ammonia/diesel mixtures can be reproduced by this new mechanism, but the new mechanism fails to reproduce the NTC behavior and first-stage IDTs. The kinetic analysis indicates that  $\text{NH}_2 + \text{NO} = \text{N}_2 + \text{H}_2\text{O}$  and  $\text{NH}_3 + \text{OH} = \text{NH}_2 + \text{H}_2\text{O}$  are crucial for accurately predicting IDTs. An experimental and numerical study was conducted by Dong et al. [27] to investigate the IDTs of ammonia/n-heptane mixtures. The reactivity of ammonia/n-heptane mixtures is significantly impacted by the ammonia blending ratio and oxygen concentration. They developed a new mechanism based on existing mechanisms. The new mechanism can reproduce the IDTs of ammonia/n-heptane mixtures in extensive conditions. Sensitivity and flux analyses indicated that reactions  $\text{NC}_7\text{H}_{16} + \text{NH}_2$  are crucial for the ignition process of ammonia/diesel mixtures. An experimental and numerical study was conducted to investigate the IDTs of ammonia/diesel mixtures, with ammonia substitutions ranging from 20% to 90% [28]. The significant two-stage ignition and NTC behavior only occur when the amount of diesel exceeds a certain value. They also found that the first-stage IDTs and total IDTs of ammonia/diesel fuel blends are prolonged with an increase in the ammonia energy fraction. Then, they developed a new dual-fuel mechanism to simulate the ignition mechanism in which the interaction pathways between diesel and ammonia are included. This mechanism has a better performance in predicting IDTs compared to the original mechanism. However, the new mechanism still fails to predict the IDTs of NTC regime at an ammonia energy fraction of 20%. Sensitivity and rate of production (ROP) analyses illustrate that the overprediction of IDTs for ammonia/diesel mixtures is mainly due to rate coefficient of  $\text{NO} + \text{HO}_2 = \text{NO}_2 + \text{OH}$ . NO will accelerate the conversion of  $\text{HO}_2$  to OH, which will greatly shorten the IDTs of ammonia/diesel mixtures. The new mechanism does not include interactions between N-containing species (NO,  $\text{NO}_2$ , and  $\text{NH}_2$ ) and NTC-related species, which may lead to the inaccurate prediction of IDTs in the NTC regime. Then, they investigated the IDTs of ammonia/diesel mixtures [29]. An increase in the equivalence ratio, energy fraction of diesel, and oxygen concentration shortened the IDTs of ammonia/diesel fuel blends. They also found that the reaction  $\text{RH} + \text{NH}_2 = \text{R} + \text{NH}_3$  is crucial for the prediction of the IDTs of ammonia/diesel mixtures at high pressure. The rate coefficients of  $\text{NO} + \text{HO}_2 = \text{NO}_2 + \text{OH}$  and  $2\text{OH} (+\text{M}) = \text{H}_2\text{O}_2 (+\text{M})$  are crucial for predicting the trend of IDTs with pressure variation, and the reaction rates of these two reactions rise with increases in the pressure. The influence of the oxygen concentration on the IDTs is closely related to  $\text{H}_2\text{NO} + \text{O}_2 = \text{HNO} + \text{HO}_2$ . Wen et al. [30] found that the ignition of ammonia near walls is mainly characterized by orange chemiluminescence in the combustion of  $\text{NH}_3/\text{NC}_7\text{H}_{16}$  mixtures. The influence of ambient temperature on the IDTs of  $\text{NH}_3/\text{NC}_7\text{H}_{16}$  mixtures is greater than that of ambient pressure. Thorsen et al. [31] found that rate parameters of  $\text{NH}_2 + \text{HO}_2$  and  $\text{NH}_2 + \text{NC}_7\text{H}_{16}$  are crucial for predicting the IDTs for  $\text{NH}_3/\text{NC}_7\text{H}_{16}$  mixtures at high pressure. Song et al. [32] investigated the IDTs of ammonia/diesel mixtures at a low n-heptane blending ratio in an RCM. They found that the IDTs of ammonia are significantly shortened by adding a small amount of n-heptane. A newly developed dual-fuel mechanism was constructed to simulate the IDTs of  $\text{NH}_3/\text{NC}_7\text{H}_{16}$  mixtures. The numerical study found that the consumption of  $\text{NC}_7\text{H}_{16}$  happens prior to that of ammonia. The reaction  $\text{NH}_2 + \text{NC}_7\text{H}_{16}$  is the main consumption pathway of  $\text{NC}_7\text{H}_{16}$  at a low n-heptane mass fraction. The reactions between  $\text{NH}_3$  and OH have the greatest inhibitory effect on ignition. The reaction  $\text{O}_2 + \text{NH}_3 = \text{NH}_2 + \text{HO}_2$  is crucial to extend the NTC regime of  $\text{NH}_3/\text{NC}_7\text{H}_{16}$  mixtures at different n-heptane mass fractions and different equivalence ratios. Huang et al. [33]

studied the ignition performance of  $\text{NH}_3/\text{NC}_7\text{H}_{16}$  mixtures with ammonia energy fractions of 0%, 20%, and 40%. In all research on energy fractions, both the first-stage IDTs and total IDTs are prolonged with increases in the ammonia energy ratio. Li et al. [34] found that the IDTs increase exponentially with the increases in the ammonia blending fraction. At 1200 K, the consumption rate of ammonia shows a parabolic relationship with the concentration of OH. As the concentration of ammonia increases, the ignition core increases.  $\text{OH} + \text{NH}_3 = \text{H}_2\text{O} + \text{NH}_2$  exhibits positive sensitivity to the IDTs when the ammonia energy fraction is less than 10%, and negative sensitivity when the ammonia energy fraction is greater than 10%. Li et al. [34] performed a numerical investigation to study the IDTs of ammonia/n-heptane mixtures. It was found that only temperature has a significant effect on the IDTs of  $\text{NH}_3/\text{NC}_7\text{H}_{16}$  mixtures in all research conditions, whereas the influence of the pressure, equivalence ratio, and ammonia mass fraction is obvious in limited conditions. The rate of consumption and production (ROP) analysis indicated that the temperature increasing from the low to the medium temperature stage is mainly due to the combustion of n-heptane, while the temperature increasing from the medium to the high temperature stage is mainly due to the combustion of ammonia. Extensive studies have been conducted on the IDTs of  $\text{NH}_3/\text{NC}_7\text{H}_{16}$  mixtures, and the interaction mechanism between the ammonia and diesel ignition has been preliminarily explored from the perspective of elementary reactions. However, these studies have failed to reveal the thermal effect and the chemical effect of diesel on the IDTs of ammonia.

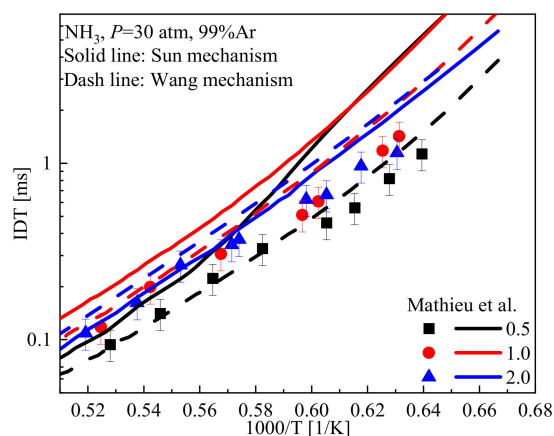
The aim of the current study is to analyze the thermal effect and the chemical effect of diesel on the IDTs of ammonia under different conditions. ROP and sensitivity analyses will be conducted to reveal the mechanism of the influence of the thermal effect and the chemical effect on the IDTs of ammonia under different conditions. The present research results will provide important theoretical guidance for deepening our understanding of the interaction between diesel/ammonia dual-fuels and the combustion process of ammonia/diesel dual-fuel engines.

## 2. Numerical Method

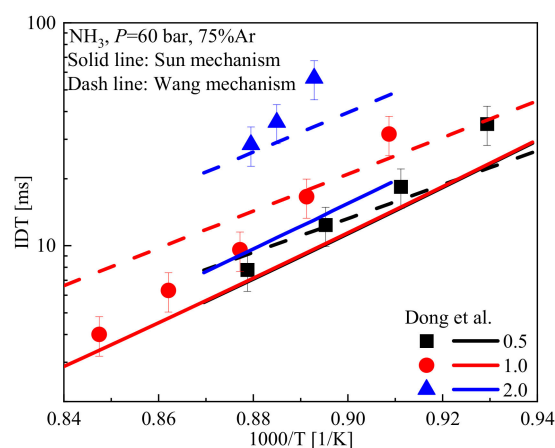
The current investigation is performed on a closed homogeneous reaction model with an adiabatic temperature boundary condition in Ansys Chemkin 18.0 software. The ignition delay time (IDT) is defined as the time interval from the beginning to the moment that the OH concentration change rate reaches its maximum. The initial temperature, equivalence ratio, fuel ratio, and pressure are determined based on the initial conditions at the compression top dead center of the compression ignition engine. Two ammonia/n-heptane dual-fuel mechanisms are collected and further verified under extensive conditions, and the mechanisms include: (a) Sun mechanism [35] and (b) Wang mechanism [36].

Figure 1 shows a comparison of the calculated IDTs of  $\text{NH}_3$  and the experimental data from Mathieu et al. [37] at equivalence ratios of 0.5, 1.0, and 2.0. At  $\Phi = 0.5$ , the IDTs calculated by the Wang mechanism are in good agreement with the experimental data, whereas the Sun mechanism overpredicted the IDTs at low and medium temperatures. At  $\Phi = 1.0$ , the Wang mechanism has a good performance in predicting the IDTs of  $\text{NH}_3$  at high temperatures, and slightly overpredicts the IDTs at low and medium temperatures. However, the Sun mechanism greatly overestimates the IDTs of  $\text{NH}_3$ . At  $\Phi = 2.0$ , the IDTs calculated by the Sun mechanism agree well with the IDTs of  $\text{NH}_3$  measured by Mathieu et al. [37] at medium and high temperatures and slightly overestimate the IDTs of  $\text{NH}_3$  measured by Mathieu et al. [37] at low temperatures, whereas the Wang mechanism slightly overestimates the IDTs. Figure 2 depicts the comparison of the calculated IDTs of ammonia and the measured IDTs from Dong et al. [27] under equivalence ratios of 0.5, 1.0, and 2.0. The Wang mechanism has a good performance in the prediction of the IDTs of ammonia at medium and high temperatures, and slightly insufficient predictions at low temperatures when the equivalence ratio is 0.5. The Wang mechanism has a good performance in predicting the IDTs at low temperatures, and slightly overpredicts at medium and high temperatures when the equivalence ratio is 1.0. The Wang mechanism

has good performance in predicting the IDTs of ammonia at high temperatures, and slightly overpredicts at low and medium temperatures when the equivalence ratio is 2.0. The IDTs calculated by the Sun mechanism are slightly lower than the measured IDTs at  $\Phi = 0.5$ , and much higher than the measured IDTs at  $\Phi = 1.0$  and  $\Phi = 2.0$ . Note that the IDTs predicted by the Sun mechanism are almost the same at  $\Phi = 0.5$  and  $\Phi = 1.0$ .

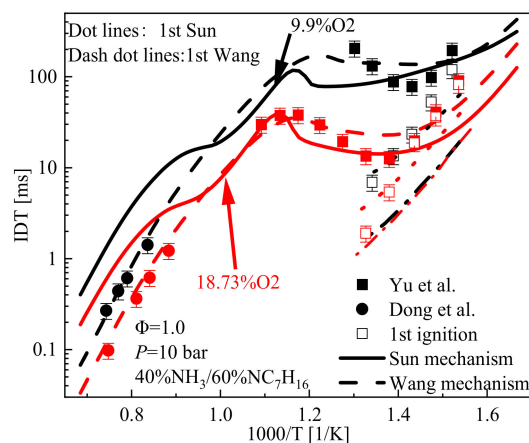


**Figure 1.** The comparison of the calculated IDTs of ammonia and measured IDTs from Mathieu et al. [37] at  $p = 30$  atm, a dilution rate of 99%, and different equivalence ratios.



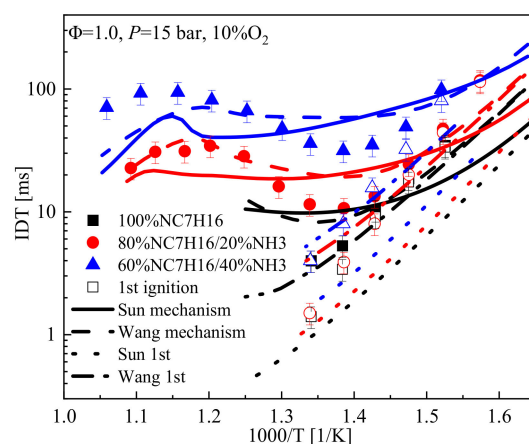
**Figure 2.** The comparison of the calculated IDTs of ammonia and measured IDTs from Dong et al. [27] at  $p = 60$  bar, a dilution rate of 75%, and different equivalence ratios.

Figure 3 depicts the calculated and measured [26,27] IDTs of  $\text{NH}_3/\text{NC}_7\text{H}_{16}$  mixtures at different oxygen concentrations. The Wang mechanism has good performance in predicting the IDTs of  $\text{NH}_3/\text{NC}_7\text{H}_{16}$  mixtures at most research temperatures when the oxygen concentration is 9.9% and 18.7%. At an oxygen concentration of 9.9%, the Sun mechanism has good performance in the prediction of the IDTs at low temperatures, but insufficient predictions at medium temperatures and overly high predictions at high temperatures. At an oxygen concentration of 18.7%, the Sun mechanism only has a good performance in predicting the IDTs of  $\text{NH}_3/\text{NC}_7\text{H}_{16}$  mixtures at medium temperatures. The Wang mechanism has a good performance in predicting the first-stage IDTs at oxygen concentrations of 9.9% and 18.7%. The first-stage IDTs predicted by the Sun mechanism only agree well with the measured first-stage IDTs at high temperatures when the oxygen concentration is 18.7%, and predicts lower than the experimental data under other conditions.



**Figure 3.** The comparison of the calculated IDTs of  $\text{NH}_3/\text{NC}_7\text{H}_{16}$  fuel blends and measured IDTs from Yu et al. [26] and Dong et al. [27] at  $p = 10$  bar,  $\Phi = 1.0$ , a n-heptane mass fraction of 60%, and different oxygen concentrations.

Figure 4 shows that, at all three n-heptane energy ratios, the predicted IDTs of both mechanisms can only partially match the experimental data [26,27], but the Wang mechanism has a better performance in predicting the IDTs of  $\text{NH}_3/\text{NC}_7\text{H}_{16}$  mixtures over the entire temperature range. The Wang mechanism also has better performance in predicting first-stage IDTs for the three mixtures.



**Figure 4.** The comparison of the calculated IDTs of  $\text{NH}_3/\text{NC}_7\text{H}_{16}$  fuel blends and measured IDTs from Yu et al. [26] and Dong et al. [27] at  $p = 15$  bar,  $\Phi = 1.0$ , an oxygen concentration of 10%, and different n-heptane mass fractions.

Based on the above comparison, the Wang mechanism is able to predict the ignition characteristics of  $\text{NH}_3/\text{NC}_7\text{H}_{16}$  mixtures. Moreover, the Wang mechanism has been successfully validated and used to simulate the IDTs of  $\text{NH}_3/\text{NC}_7\text{H}_{16}$  mixtures in direct numerical simulations in a previous study [33]. Therefore, the Wang mechanism is applied to simulate the IDTs of  $\text{NH}_3/\text{NC}_7\text{H}_{16}$  mixtures in the present study.

To decouple the thermal effect and the chemical effect of n-heptane on the ignition process of ammonia, the isotope labeling method is applied in the present study. The isotope labeling method uses the isotope D of H to represent the hydrogen element in ammonia, assuming that D does not react with n-heptane. To eliminate the influence of the chemical effect from the ignition of n-heptane, the hydrogen element in ammonia is represented by D. Moreover, O radical is produced in the oxidation of n-heptane, which has a high activity and can promote better IDTs of ammonia. The oxygen reacting with  $\text{ND}_3$  is labeled as G to eliminate the influence of the O radical. By comparing the IDTs of  $\text{NH}_3$  reacting with  $\text{G}_2$  and  $\text{O}_2$ , the influence of the O radical from the oxidation of n-heptane can

be decoupled.  $\text{NC}_7\text{H}_{16}/\text{NH}_3$  represents the group with the chemical effect + the thermal effect,  $\text{NC}_7\text{H}_{16}/\text{ND}_3$  represents the group with the thermal effect + the effect of O radical, and  $\text{NC}_7\text{H}_{16}/\text{ND}_3\text{-G}$  represents the group with only the thermal effect.

The setting of initial conditions is based on the ignition conditions of internal combustion engines. The initial temperature, pressure, equivalence ratio, and n-heptane mass fraction are set in the ranges of 800~1200 K, 20~100 bar, 0.5~2.0, and 10~30%, respectively.

### 3. Result and Discussion

#### 3.1. Decoupling the Chemical Effect and the Thermal Effect on IDTs

The NTC behavior of the IDTs of n-heptane has been proven, whereas it has been not found in the IDTs of ammonia. The NTC behavior will be significantly affected by the blending of ammonia. Figure 5 shows that, at a n-heptane mass fraction of 10%, the NTC behavior only exists in  $\text{NC}_7\text{H}_{16}/\text{ND}_3\text{-G}$  at low temperatures and an initial pressure of 20 atm. At  $p = 20$  bar, the IDTs of ammonia are greatly shortened by the chemical effect of n-heptane at low temperatures, but slightly prolonged at medium temperatures and almost identical at high temperatures. The effect of the O radical has a significant promoting effect on the IDTs of  $\text{NH}_3$  at low temperatures, and the promoting effect decreases when the temperature increases. The oxidation rate of ammonia is relatively slow at low temperatures, and O radical derived from the ignition of n-heptane will accelerate the oxidation of ammonia; thereby, the IDT is shortened. The reaction rate of ammonia increases with increases in the temperature, and the effect of O radical is weakened. At  $p = 50$  bar, the IDTs of ammonia are significantly shortened by the chemical effect at low temperatures, and the influence of the chemical effect decreases when the temperature increases. At high temperatures, the chemical effect becomes negligible. At an initial pressure of 100 bar, the influence of the chemical effect on the IDTs of ammonia follows a similar pattern to that at 50 bar. In addition, the promoting effect of the chemical effect on the IDTs of ammonia decreases when the pressure increases at low temperatures. At initial pressures of 50 bar and 100 bar, the effect of O radical is similar to that at 20 bar, and this promoting effect on the IDTs of ammonia gradually weakens with the increases in temperature.

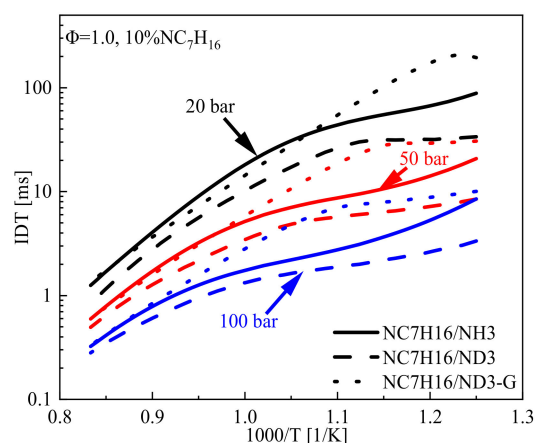


**Figure 5.** Predicted IDTs of  $\text{NH}_3/\text{NC}_7\text{H}_{16}$  mixtures at a n-heptane mass fraction of 10%,  $\Phi = 1.0$ , and different pressures.

With the equivalence ratio decreasing or increasing, the influence of the chemical effect increases over the entire temperature range, as shown in Figure 6. At  $\Phi = 0.5$ , the promoting effect of the chemical effect on the IDTs of  $\text{NH}_3$  decreases when the temperature increases. At  $\Phi = 2.0$ , the promoting effect of the chemical effect first increases and then decreases when the temperature increases. The promoting effect of O radical is significantly reduced at a low equivalence ratio, and the promoting effect decreases when the temperature increases. At  $\Phi = 2.0$ , the promotional effect of O radical is enhanced. The promotional effect of O radical decreases with the increase in temperature, and the NTC behavior

is observed in the IDTs of  $\text{NH}_3/\text{NC}_7\text{H}_{16}$  mixtures under the thermal effect + the effect of O radical.

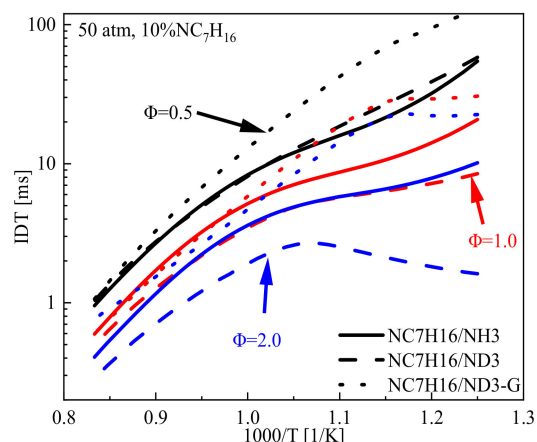


**Figure 6.** Predicted IDTs of  $\text{NH}_3/\text{NC}_7\text{H}_{16}$  mixtures at a n-heptane mass fraction of 10%,  $p = 50$  bar, and different equivalence ratios.

Figure 7 illustrates the IDTs of  $\text{NH}_3/\text{NC}_7\text{H}_{16}$  mixtures at different n-heptane mass fractions. When the n-heptane mass fraction increases, the effect of the chemical effect of  $\text{NC}_7\text{H}_{16}$  on the ignition of  $\text{NH}_3$  is reduced. At a n-heptane mass fraction of 20%, the chemical effect has an inhibitory effect on the IDTs of  $\text{NH}_3$  at low and high temperatures, but it turns to a promoting effect at medium temperatures. At a n-heptane mass fraction of 30%, the influence of the chemical effect on the IDTs of ammonia is similar to that at a n-heptane mass fraction of 20%. When the n-heptane mass fraction increases from 10% to 20%, the promoting effect of O radical is enhanced at low and high temperatures, but weakened at medium temperatures. When the n-heptane mass fraction increases to 30%, the promoting effect of O radical is weakened throughout the entire temperature range. Furthermore, obvious NTC behavior exists at n-heptane mass fractions of 20% and 30%. The O radical pushes the NTC behavior towards a higher temperature at n-heptane mass fractions of 20% and 30%.

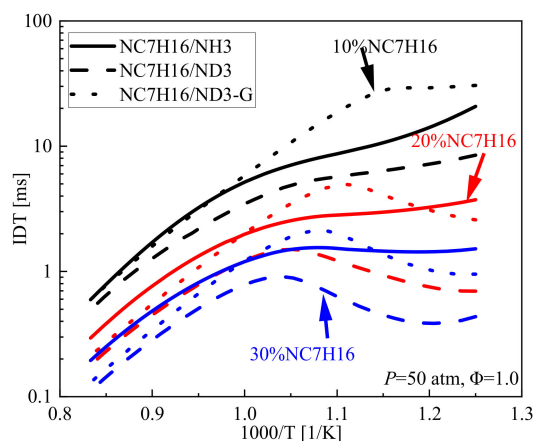


**Figure 7.** Predicted IDTs of  $\text{NH}_3/\text{NC}_7\text{H}_{16}$  mixtures at  $p = 50$  bar,  $\Phi = 1.0$ , and different n-heptane mass fractions.

Figure 8 shows that, at  $\Phi = 0.5$ , the impact of the chemical effect on the IDTs of  $\text{NH}_3$  decreases when the n-heptane mass fraction increases. When the n-heptane mass fraction is 20%, the chemical effect has a promotional effect on the IDTs at low and medium temperatures, while it has an inhibitory effect on the IDTs at high temperatures. When the n-heptane mass fraction is 30%, the promoting effect of the chemical effect only occurs at



medium temperatures. O radical has a significant promoting effect at low temperatures, and this promoting effect decreases when the temperature increases. Furthermore, the promoting effect of O radical is weakened with increases in the n-heptane mass fraction. The NTC behavior is only observed in the IDTs of  $\text{NC}_7\text{H}_{16}/\text{ND}_3$  and  $\text{NC}_7\text{H}_{16}/\text{ND}_3\text{-G}$  at a n-heptane mass fraction of 30%.

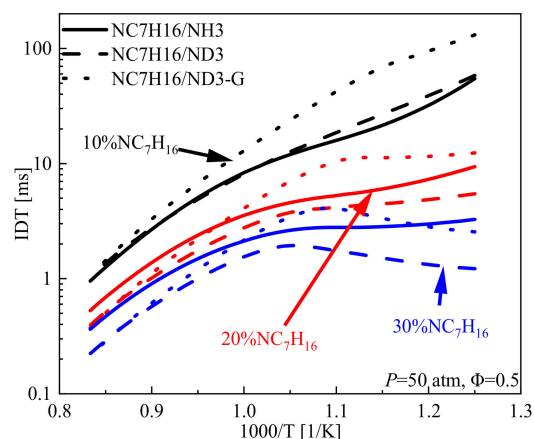


**Figure 8.** Predicted IDTs of  $\text{NH}_3/\text{NC}_7\text{H}_{16}$  mixtures at  $p = 50$  bar,  $\Phi = 0.5$ , and different n-heptane mass fractions.

### 3.2. Chemical Kinetic Analysis

Figures 9 and 10 show the time evolution of fuels at equivalence ratios of 0.5 and 1.0. For all of the cases, the consumption of n-heptane happens before that of ammonia, the rapid consumption of ammonia occurs at the ignition timing, and the n-heptane is completely consumed before the ignition timing. At all temperatures and equivalence ratios, the n-heptane of  $\text{NC}_7\text{H}_{16}/\text{NH}_3$  is almost not consumed during the initial period. The consumption rate of n-heptane gradually increases after it begins to be consumed. The consumption of n-heptane for  $\text{NC}_7\text{H}_{16}/\text{NH}_3$  happens prior to that of ammonia. The consumption rate of ammonia is relatively low before the n-heptane is completely consumed, and the ammonia is rapidly consumed at the ignition time. Figures 9 and 10 show that, at 800 K, both the chemical effect and the effect of the O radical can advance the rapid consumption of ammonia. Figures 9a,b and 10a,b show that, under only the thermal effect, the consumption of n-heptane can be classified into three stages: (a) almost no consumption stage, (b) rapid consumption stage, and (c) slow consumption stage at 800 K. Due to the influence of the chemical effect, the rapid consumption stage of n-heptane disappears, while the consumption rate of the slow consumption stage gradually increases. In addition, the depletion of n-heptane occurs at a later time. O radical can advance the rapid consumption stage of n-heptane, but weakens the slow consumption stage. As the n-heptane mass fraction increases, the beginning time of the rapid consumption of ammonia and n-heptane is advanced. Figures 9c,d and 10c,d depict that, with the temperature increasing to 900 K, the time of the rapid consumption stage of n-heptane for  $\text{NC}_7\text{H}_{16}/\text{ND}_3\text{-G}$  is decreased, and it is only observed at a n-heptane mass fraction of 30%. The chemical effect can further reduce the consumption rate of n-heptane, and retard the time at which n-heptane is depleted. O radical can enhance the rapid consumption stage of n-heptane, but weakens the slow consumption stage. Figures 9e,f and 10e,f illustrate that, at 1100 K, the rapid consumption stage of n-heptane for  $\text{NC}_7\text{H}_{16}/\text{ND}_3\text{-G}$  completely disappears, and the chemical effect reduces the consumption rate of n-heptane in the rapid consumption stage, while O radical enhances the consumption rate of n-heptane. Note that the chemical effect can advance the time at which n-heptane starts to be consumed.

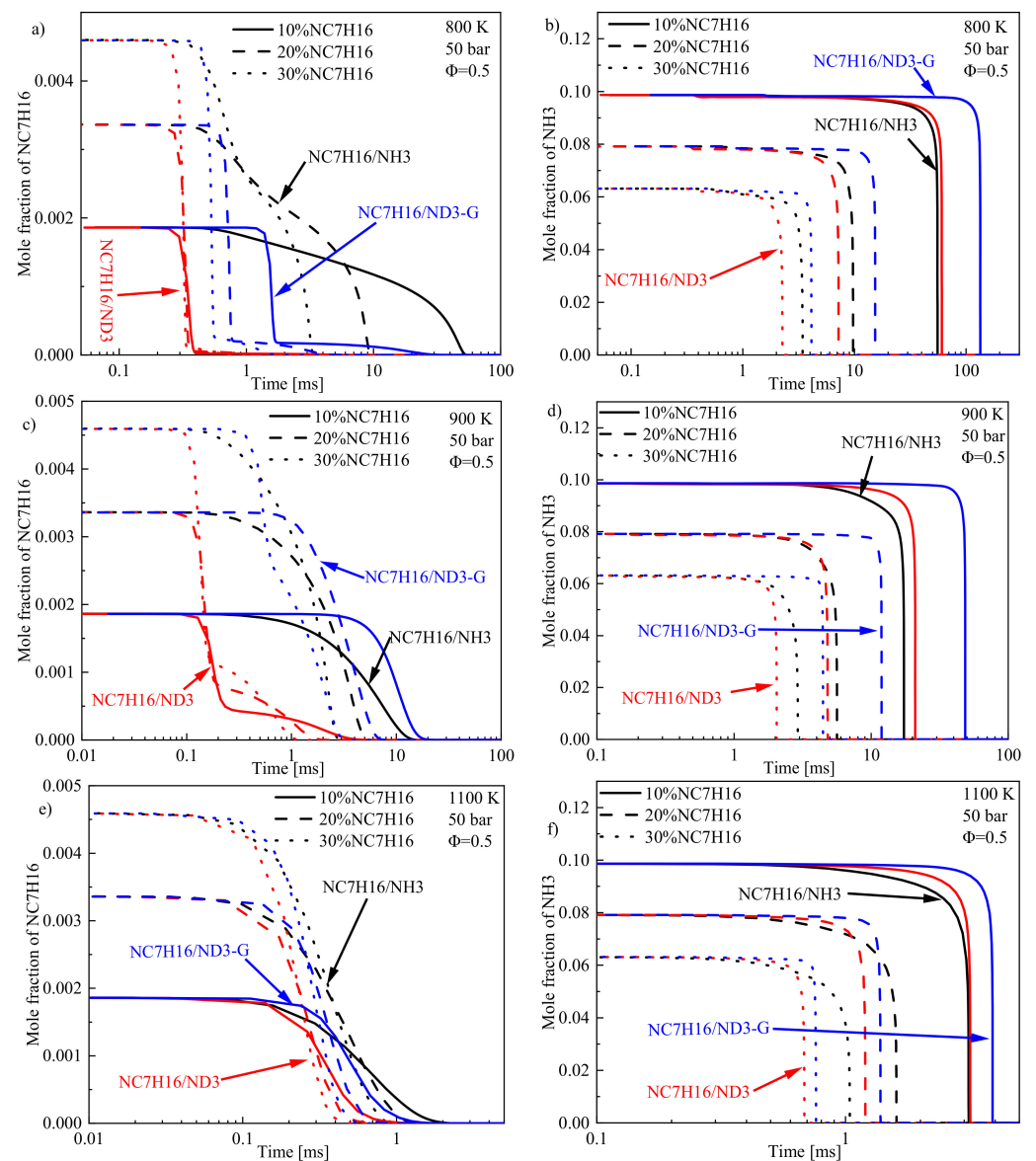


**Figure 9.** Time evolution of  $\text{NH}_3$  and  $\text{NC}_7\text{H}_{16}$  at n-heptane mass fractions of 10%, 20%, and 30%,  $\Phi = 0.5$  and  $p = 50$  bar, (a) 800 K, time evolution of  $\text{NC}_7\text{H}_{16}$ , (b) 800 K, time evolution of  $\text{NH}_3$ , (c) 900 K, time evolution of  $\text{NC}_7\text{H}_{16}$ , (d) 900 K, time evolution of  $\text{NH}_3$ , (e) 1100 K, time evolution of  $\text{NC}_7\text{H}_{16}$ , and (f) 1100 K, time evolution of  $\text{NH}_3$ .

Figures 11 and 12 depict the evolution over time of the temperature of n-heptane/ammonia fuel blends at  $\Phi = 0.5$  and  $\Phi = 1.0$ . Figures 11a and 12a show that there are two rapid increase stages of the temperature in  $\text{NC}_7\text{H}_{16}/\text{ND}_3\text{-G}$  at 800 K. The first rapid increase stage happens owing to the rapid consumption of n-heptane, while the second rapid increase stage happens owing to the rapid consumption of ammonia. The chemical effect weakens the rapid consumption stage of n-heptane; therefore, it also weakens the first rapid increase stage of the temperature for  $\text{NC}_7\text{H}_{16}/\text{NH}_3$ . O radical can enhance the rapid consumption stage of n-heptane; therefore, the first rapid increase stage of temperature is enhanced. Figures 11b and 12b illustrate that the first rapid increase stage of temperature for  $\text{NC}_7\text{H}_{16}/\text{ND}_3\text{-G}$  disappears at 900 K. The chemical effect can improve the initial rise rate of the temperature, and O radical leads to the first rapid increase stage of the temperature. Figures 11c and 12c show that the chemical effect leads to a lower initial rise rate of the temperature owing to the lower consumption rate of n-heptane, whereas O radical leads to a higher initial rise rate of the temperature owing to the higher oxidation rate of n-heptane.

Note that the adiabatic flame temperature of the three cases is almost the same. The temperature increasing during the ignition of  $\text{NH}_3/\text{NC}_7\text{H}_{16}$  mixtures is mainly contributed by the oxidation of ammonia.

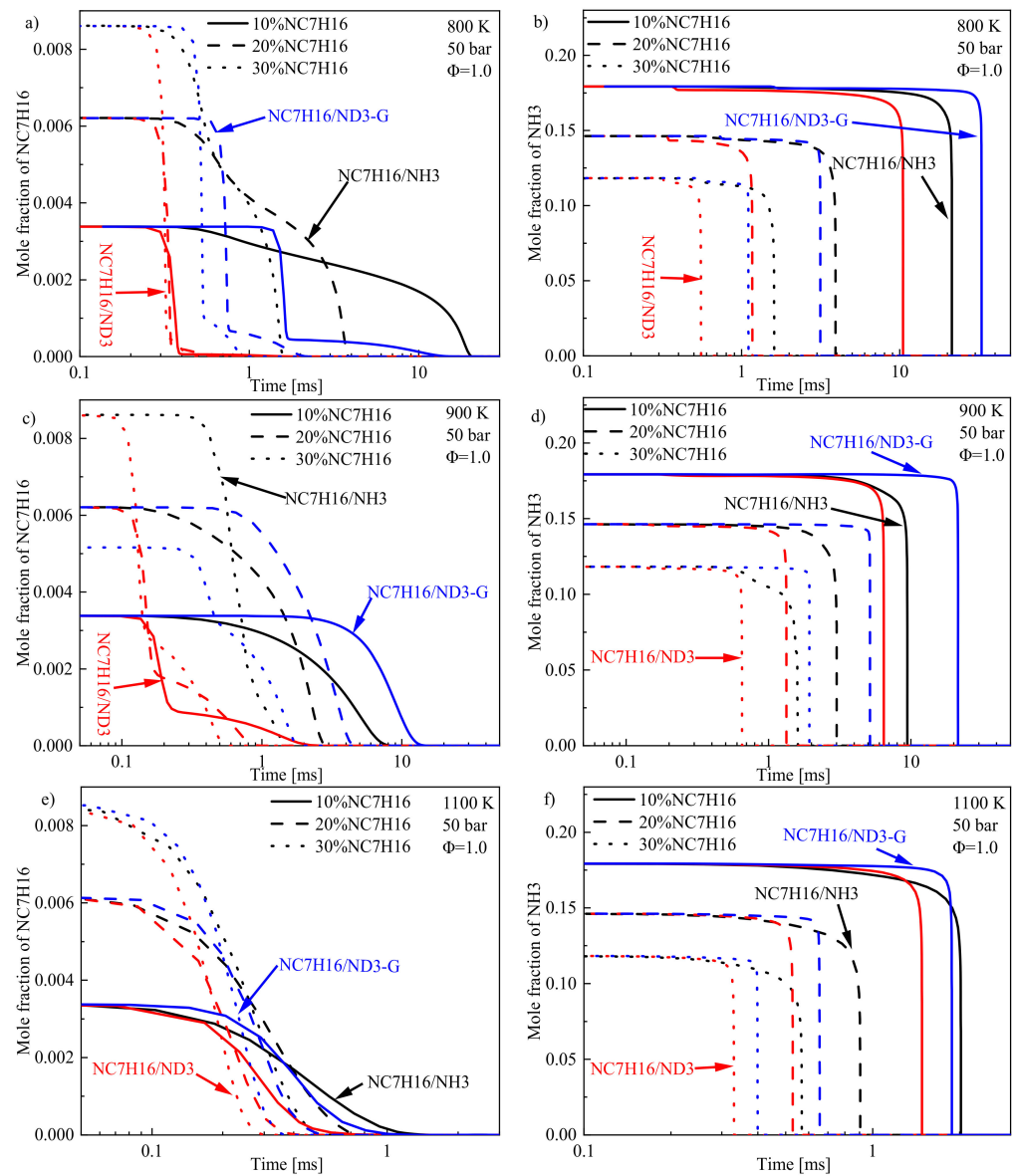


**Figure 10.** Time evolution of  $\text{NH}_3$  and  $\text{NC}_7\text{H}_{16}$  at n-heptane mass fractions of 10%, 20%, and 30%,  $\Phi = 1.0$  and  $p = 50$  bar, (a) 800 K, time evolution of  $\text{NC}_7\text{H}_{16}$ , (b) 800 K, time evolution of  $\text{NH}_3$ , (c) 900 K, time evolution of  $\text{NC}_7\text{H}_{16}$ , (d) 900 K, time evolution of  $\text{NH}_3$ , (e) 1100 K, time evolution of  $\text{NC}_7\text{H}_{16}$ , and (f) 1100 K, time evolution of  $\text{NH}_3$ .

Rate of consumption and production (ROP) analysis is an important method in understanding the mechanism of the ignition and combustion of  $\text{NH}_3/\text{NC}_7\text{H}_{16}$  mixtures. O radical is an important species for the decoupling analysis of the ignition characteristics of  $\text{NH}_3/\text{NC}_7\text{H}_{16}$  mixtures. The reactions used in the ROP analysis are listed in Table 1.

Figures 13–15 show the ROPs of O radicals at different temperatures and n-heptane mass fractions. Figures 13a–c and 14a–c show that, when the n-heptane mass fraction is 10% and 20%, the main consumption or production reactions of O radical for the three groups are the same at various temperatures. However, the ROPs of the O radical for  $\text{NC}_7\text{H}_{16}/\text{ND}_3$  are slightly different from those of  $\text{NC}_7\text{H}_{16}/\text{NH}_3$  and  $\text{NC}_7\text{H}_{16}/\text{ND}_3\text{-G}$  at a n-heptane mass fraction of 30%. In  $\text{NC}_7\text{H}_{16}/\text{NH}_3$ , R10 and R12 are the reactions associated with both n-

heptane and ammonia, while, in  $\text{NC}_7\text{H}_{16}/\text{ND}_3$  and  $\text{NC}_7\text{H}_{16}/\text{ND}_3\text{-G}$ , R10 and R12 are the reactions associated with n-heptane and G10 and G12 are the reactions related to ammonia. For all three cases, the reaction rates of R10|G10 and R12|G12 are higher than those of R230 and R249. The chemical effect has no significant promoting or inhibitory effect on R10|G10 and R12|G12, while it has an inhibitory effect on R230 and R249. Interestingly, the chemical effect can advance the maximum values of the ROPs of O radical to a lower temperature and promote the reaction rates before the maximum value occurs. The advanced effect of the chemical effect on the ROPs of the O radical increases with the increase in the n-heptane mass fraction. O radical can also advance the maximum reaction rates of ROPs to a lower temperature, but it will lead to a decrease in the maximum values of ROPs at a n-heptane mass fraction of 10%. As the n-heptane mass fraction increases, O radical still reduces the maximum reaction rates of R10|G10 and R12|G12, but enhances the maximum reaction rates of R230 and R249. Figure 15a–c shows that both R10 and G10 are the main production reactions of O radicals for  $\text{NC}_7\text{H}_{16}/\text{ND}_3$  at a n-heptane mass fraction of 30%. However, the reaction rates of R10 and R12 of  $\text{NC}_7\text{H}_{16}/\text{ND}_3\text{-G}$  are from one to two orders of magnitude lower than those of G10 and G12. This illustrates that O radical has a significant promoting effect on reactions related to n-heptane at a higher n-heptane mass fraction.

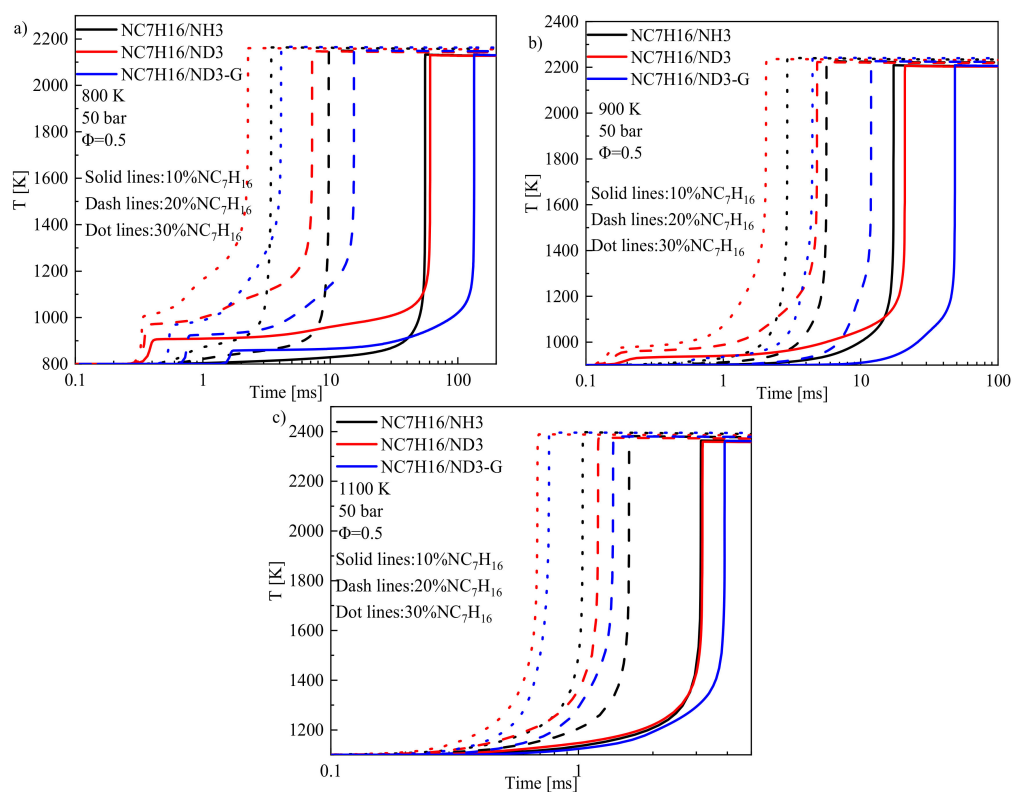


**Figure 11.** Time evolution of temperature at n-heptane mass fractions of 10%, 20%, and 30%,  $\Phi = 0.5$  and  $p = 50$  bar, (a) 800 K, (b) 900 K, and (c) 1100 K.

Figures 16–18 illustrate the ROPs of the O radical at  $\Phi = 1.0$ , different temperatures, and different n-heptane mass fractions. The main consumption and production reactions of O radical for the three cases are the same at different temperatures and n-heptane mass fractions. Figure 16a–c depicts that the chemical effect has a slight promoting effect on R10|G10 and R12|G12 at a n-heptane mass fraction of 10%, but has an inhibitory effect on R3|G3 and R230. In addition, the maximum values of ROPs for  $\text{NC}_7\text{H}_{16}/\text{NH}_3$  and  $\text{NC}_7\text{H}_{16}/\text{ND}_3\text{-G}$  occur almost at the same temperature. Figures 17a–c and 18a–c illustrate that, with the n-heptane mass fraction increasing, the promoting effect of the chemical effect on R10|G10 and R12|G12 increases, and the inhibitory effect on R230 also increases, but the inhibitory effect on R3|G3 turns into a promoting effect. The chemical effect can

advance the maximum values of ROPs to a lower temperature when the n-heptane mass fraction increases. O radical has a slight promoting effect on the ROPs at  $\Phi = 1.0$  and a n-heptane mass fraction of 10%, and the promoting effect increases with the increase in the n-heptane mass fraction.

**Table 1.** Important reactions for the ROP of  $\text{NH}_3/\text{NC}_7\text{H}_{16}$  mixtures.

Number	Reaction
R3	$\text{O} + \text{H}_2 = \text{OH} + \text{H}$
R10	$\text{O}_2 + \text{H} = \text{O} + \text{OH}$
R12	$\text{OH} + \text{OH} = \text{H}_2\text{O} + \text{O}$
R230	$\text{NH}_3 + \text{O} = \text{NH}_2 + \text{OH}/\text{ND}_3 + \text{O} = \text{ND}_2 + \text{OD}$
R249	$\text{NH} + \text{O}_2 = \text{HNO} + \text{O}/\text{ND} + \text{O}_2 = \text{DNO} + \text{O}$
G3	$\text{O} + \text{D}_2 = \text{OD} + \text{D}/\text{G} + \text{D}_2 = \text{GD} + \text{D}$
G10	$\text{O}_2 + \text{D} = \text{O} + \text{OD}/\text{O}_2 + \text{D} = \text{O} + \text{OD}$
G12	$\text{OD} + \text{OD} = \text{D}_2\text{O} + \text{O}/\text{GD} + \text{GD} = \text{D}_2\text{G} + \text{G}$

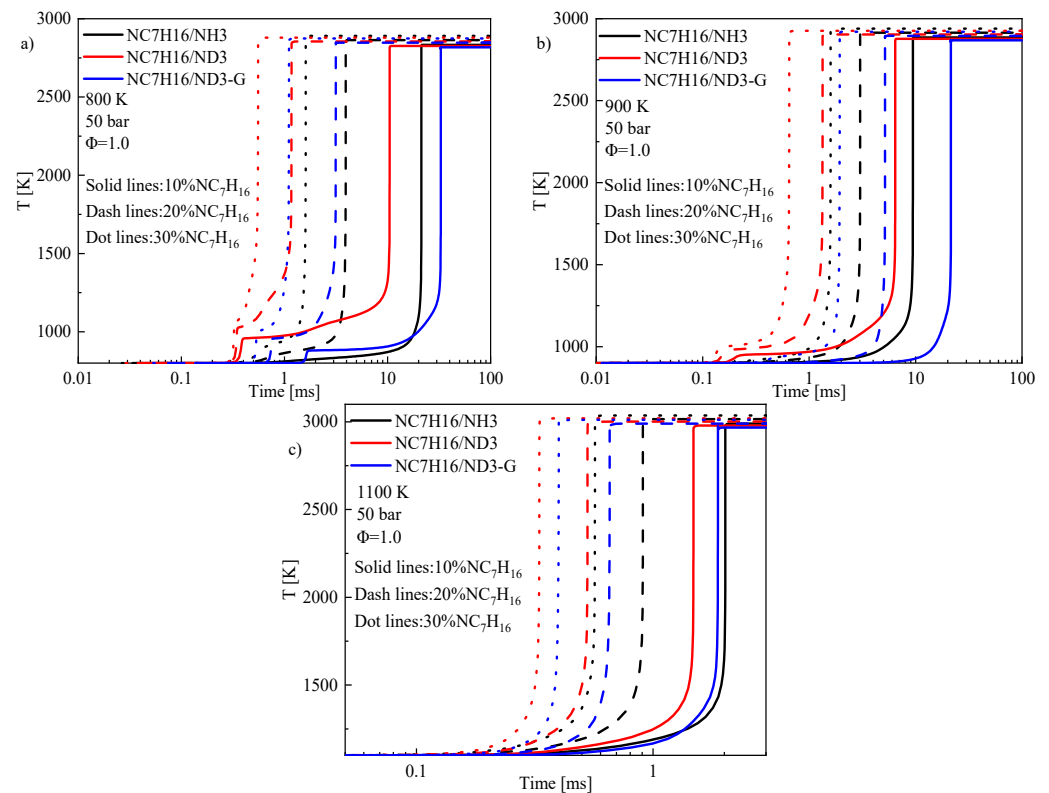


**Figure 12.** Time evolution of temperature at n-heptane mass fractions of 10%, 20%, and 30%,  $\Phi = 1.0$  and  $p = 50$  bar, (a) 800 K, (b) 900 K, and (c) 1100 K.

### 3.3. Sensitivity Analysis

To further understand the inhibitory and promoting effects of key reactions on the ignition of ammonia/n-heptane mixtures, a sensitivity analysis of the three cases was performed at different temperatures and n-heptane mass fractions to elicit further understanding of the inhibitory and promoting effects of key reactions on the IDTs of  $\text{NH}_3/\text{NC}_7\text{H}_{16}$  mixtures. The sensitivity coefficient is defined as follows:

$$S = \frac{\tau_{2k_i} - \tau_{0.5k_i}}{1.5\tau_{k_i}}$$

$\tau$  refers to the IDT, and  $k_i$  refers the rate parameter of the  $i$ -th reaction. A positive sensitivity coefficient illustrates that the reaction has an inhibitory effect on the IDTs, and

a negative sensitivity coefficient illustrates that the reaction has a promotional effect on the IDTs. The 13 reactions with the greatest impact on the IDTs of ammonia/n-heptane mixtures are selected, as shown in Table 2. The reaction can be classified into two parts: the reactions related to n-heptane (R92~178) and reactions related to ammonia (R219~337).

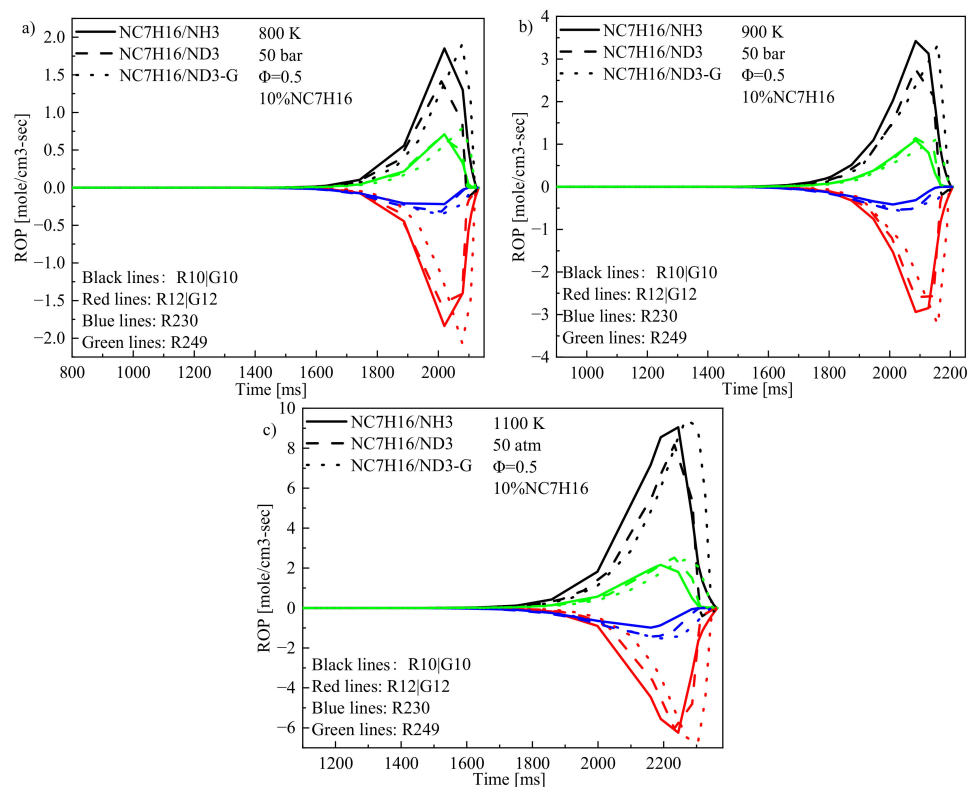


**Figure 13.** ROPs of O radical at  $\Phi = 0.5$ ,  $p = 50$  bar, a n-heptane mass fraction of 10%, (a) 800 K, (b) 900 K, and (c) 1100 K (R10|G10 means the reaction is R10 or G10, R12|G12 means the reaction is R12 or G12).

Figure 19 illustrates the sensitivity analysis of  $\text{NH}_3/\text{NC}_7\text{H}_{16}$  mixtures at a  $p = 50$  bar,  $\Phi = 0.5$ , and an n-heptane mass fraction of 10%. Figure 19a,c illustrates that the sensitivities of almost all reactions for  $\text{NC}_7\text{H}_{16}/\text{ND}_3\text{-G}$  are lower than those of  $\text{NC}_7\text{H}_{16}/\text{NH}_3$ . This indicates that the chemical effect can enhance the effects of all 13 reactions at a n-heptane mass fraction of 10%. When the n-heptane ratio is low, the temperature increase from the ignition of n-heptane is relatively small, and thus has little effect on the IDTs of ammonia, whereas even a small amount of radicals generated from the ignition of n-heptane can significantly accelerate the IDTs of ammonia. Therefore, the chemical effect can enhance the effects of all 13 reactions. Figure 19b,c depicts that the O radical has a promoting effect on the sensitivity coefficients of reactions related to ammonia. In addition, O radical has an inhibitory effect on the sensitivity coefficients of reactions related to ammonia at 800 K and 1100 K, but has a promoting effect at 900 K.

Figure 20a,c illustrates that the chemical effect has an inhibitory effect on the sensitivities of reactions associated with n-heptane at 800 K and 900 K, but has a promoting effect on those at 1100 K. The chemical effect has a promoting effect on the sensitivity coefficients of reactions related to ammonia at all three temperatures. Figure 20b,c shows that O radical has a slight inhibitory effect on the sensitivities of reactions associated with n-heptane at 800 K and 900 K, but has a promoting effect on those at 1100 K. Moreover, O radical has a slight promoting effect on the sensitivity coefficients of reactions related to ammonia. Under only the thermal effect, the sensitivities of reactions associated with n-heptane decrease with increases in the n-heptane mass fraction at 800 K and 900 K, but increase at 1100 K. The sensitivities of reactions related to ammonia decrease with increases in the n-heptane mass

fraction. Interestingly, only under the thermal effect, reactions associated with n-heptane have the greatest impact on the ignition of  $\text{NH}_3/\text{NC}_7\text{H}_{16}$  mixtures when the n-heptane mass fraction is 30%.

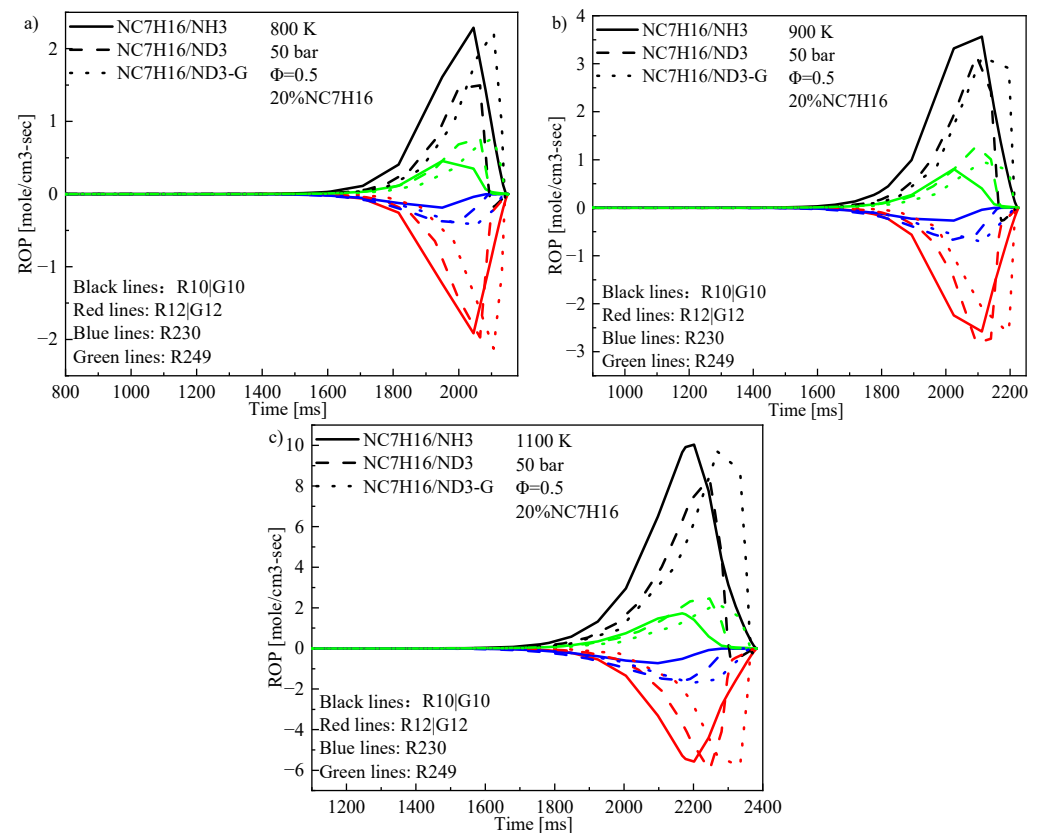


**Figure 14.** ROPs of O radical at  $\Phi = 0.5$ ,  $p = 50$  bar, a n-heptane mass fraction of 20%, (a) 800 K, (b) 900 K, and (c) 1100 K (R10|G10 means the reaction is R10 or G10, R12|G12 means the reaction is R12 or G12).

**Table 2.** Important reactions in present work.

Number	Reaction
R92	$\text{C}_2\text{H}_5 + \text{O}_2 = \text{C}_2\text{H}_4 + \text{HO}_2$
R170	$\text{NC}_7\text{H}_{16} + \text{OH} = \text{C}_7\text{H}_{15} + \text{H}_2\text{O}$
R176	$\text{C}_7\text{H}_{15}\text{O}_2 = \text{C}_7\text{H}_{14} + \text{HO}_2$
R178	$\text{C}_7\text{H}_{14}\text{OOH} + \text{O}_2 = \text{C}_7\text{H}_{14}\text{OOHO}_2$
R219	$2\text{NH}_2 (+\text{M}) = \text{N}_2\text{H}_4 (+\text{M})$
R231	$\text{OH} + \text{NH}_3 = \text{H}_2\text{O} + \text{NH}_2$
R238	$\text{NH}_3 + \text{O}_2 = \text{NH}_2 + \text{HO}_2$
R239	$\text{NH}_2 + \text{HO}_2 = \text{OH} + \text{H}_2\text{NO}$
R243	$\text{HONO} + \text{NH}_2 = \text{NH}_3 + \text{NO}_2$
R244	$\text{NO}_2 + \text{NH}_2 = \text{NO} + \text{H}_2\text{NO}$
R245	$\text{NO}_2 + \text{NH}_2 = \text{H}_2\text{O} + \text{N}_2\text{O}$
R336	$\text{NO} + \text{NH}_2 = \text{H}_2\text{O} + \text{N}_2$
R337	$\text{NO} + \text{NH}_2 = \text{OH} + \text{NNH}+$

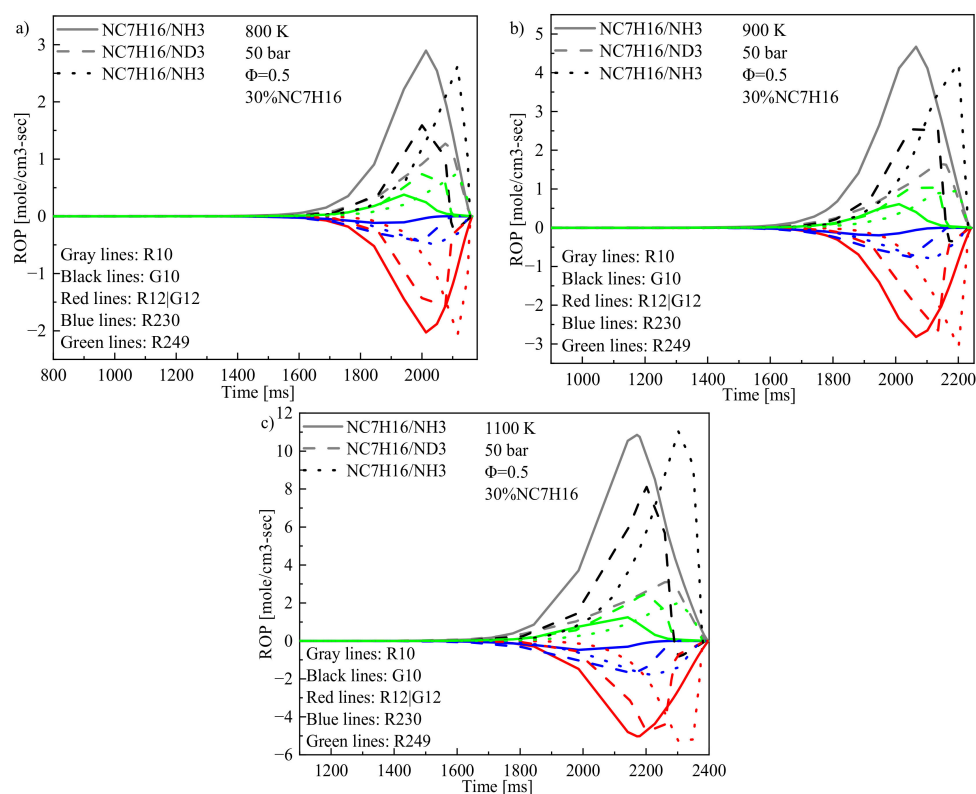


**Figure 15.** ROPs of O radical at  $\Phi = 0.5$ ,  $p = 50$  bar, and a n-heptane mass fraction of 30%, (a) 800 K, (b) 900 K, and (c) 1100 K (R12 | G12 means the reaction is R12 or G12).

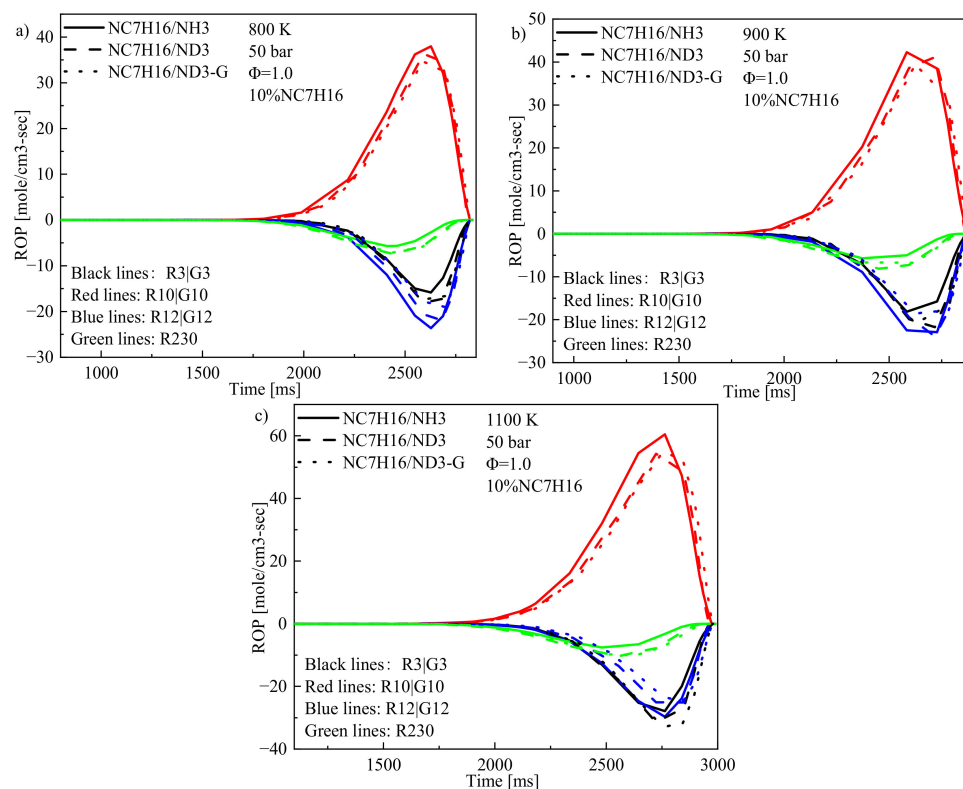


**Figure 16.** ROPs of O radical at  $\Phi = 1.0$ ,  $p = 50$  bar, and a n-heptane mass fraction of 10%, (a) 800 K, (b) 900 K, and (c) 1100 K (R3 | G3 means the reaction is R3 or G3, R10 | G10 means the reaction is R10 or G10, R12 | G12 means the reaction is R12 or G12).



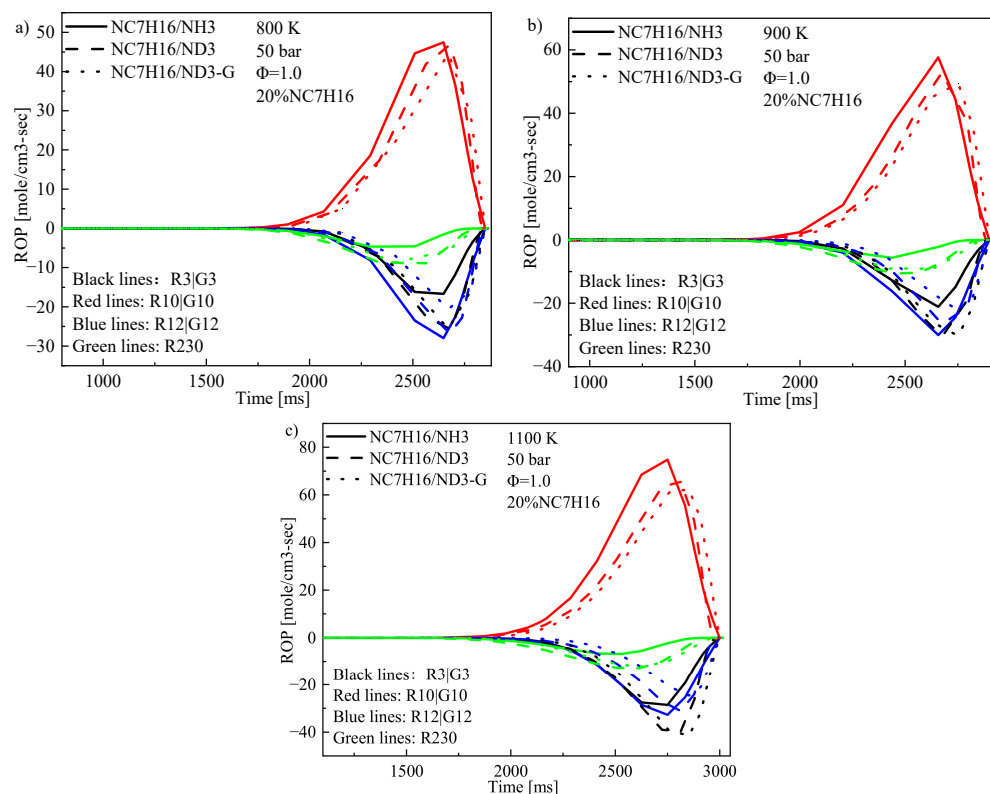


**Figure 17.** ROPs of O radical at  $\Phi = 1.0$ ,  $p = 50$  bar, and a n-heptane mass fraction of 20%, (a) 800 K, (b) 900 K, and (c) 1100 K (R3|G3 means the reaction is R3 or G3, R10|G10 means the reaction is R10 or G10, R12|G12 means the reaction is R12 or G12).

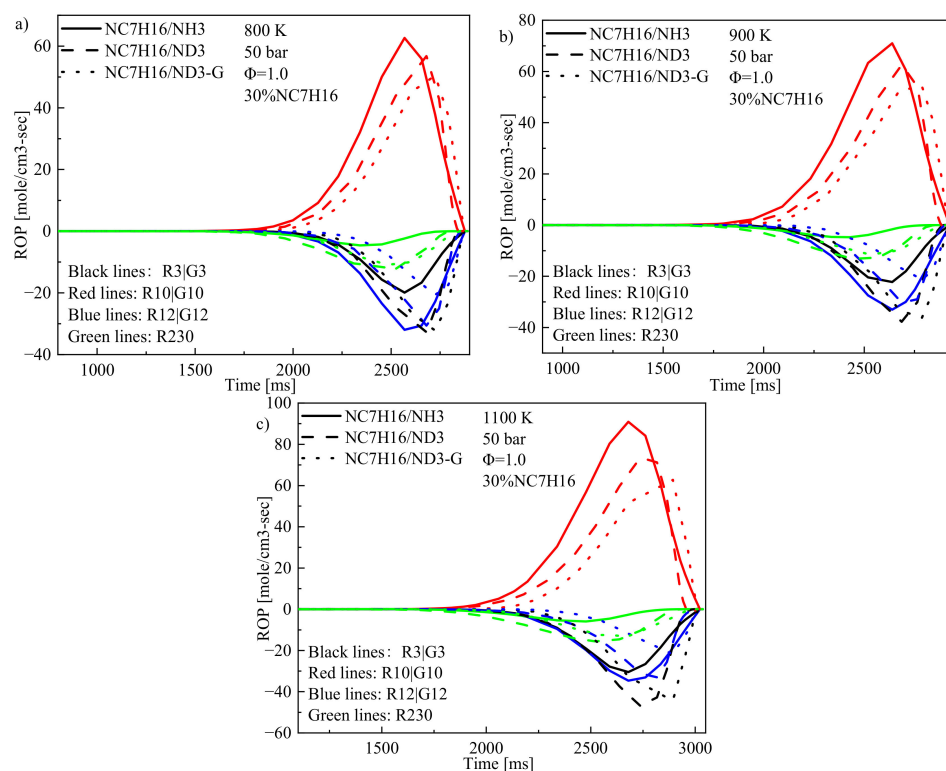


**Figure 18.** ROPs of O radical at  $\Phi = 1.0$ ,  $p = 50$  bar, and a n-heptane mass fraction of 30%, (a) 800 K, (b) 900 K, and (c) 1100 K (R3|G3 means the reaction is R3 or G3, R10|G10 means the reaction is R10 or G10, R12|G12 means the reaction is R12 or G12).

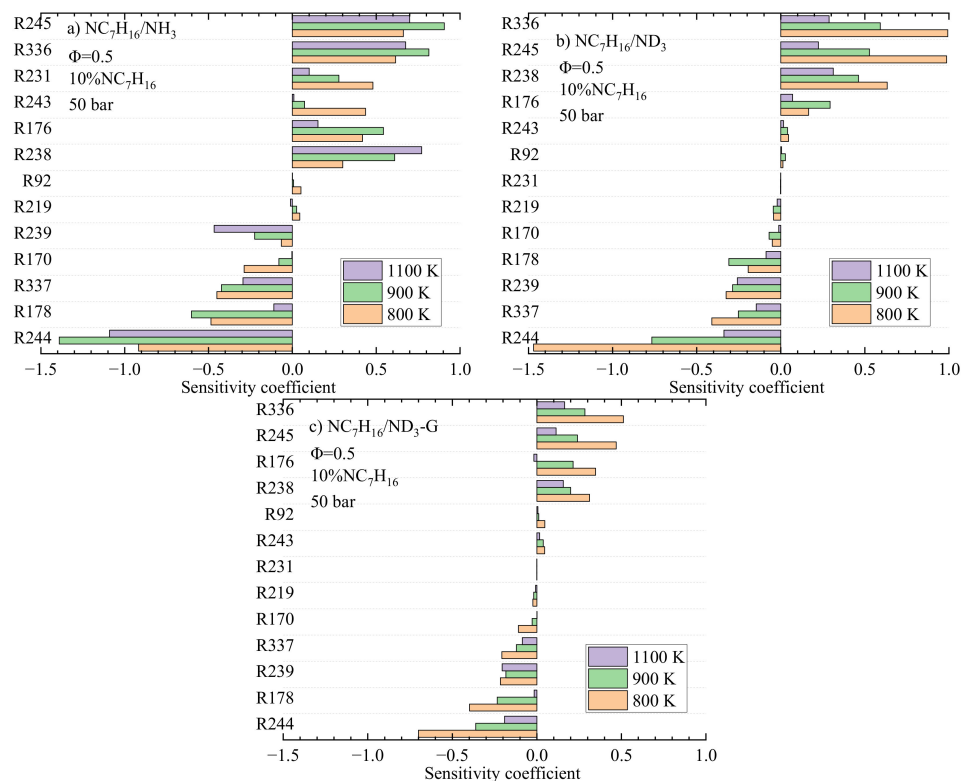


**Figure 19.** Sensitivity of IDTs for ammonia/n-heptane mixtures at 800 K, 900 K, and 1100 K,  $\Phi = 0.5$ ,  $p = 50$  bar, and a n-heptane mass fraction of 10%, (a)  $\text{NH}_3/\text{NC}_7\text{H}_{16}$ , (b)  $\text{ND}_3/\text{NC}_7\text{H}_{16}$ , and (c)  $\text{ND}_3/\text{NC}_7\text{H}_{16}\text{-G}$ .

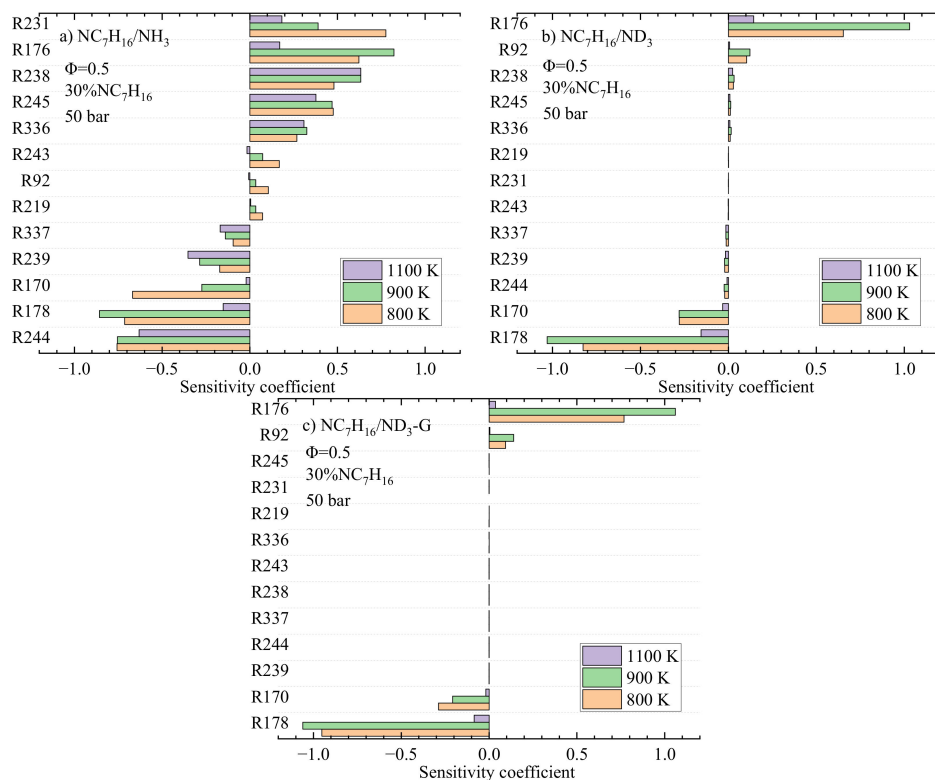


**Figure 20.** Sensitivity of IDTs for  $\text{NH}_3/\text{NC}_7\text{H}_{16}$  mixtures at 800 K, 900 K, and 1100 K,  $\Phi = 0.5$ ,  $p = 50$  bar, and a n-heptane mass fraction of 30%, (a)  $\text{NH}_3/\text{NC}_7\text{H}_{16}$ , (b)  $\text{ND}_3/\text{NC}_7\text{H}_{16}$ , and (c)  $\text{ND}_3/\text{NC}_7\text{H}_{16}\text{-G}$ .

At  $\Phi = 1.0$  and a n-heptane mass fraction of 10%, R176, R245, and R336 of  $\text{NC}_7\text{H}_{16}/\text{NH}_3$  have the greatest inhibitory effect on the IDTs of  $\text{NH}_3/\text{NC}_7\text{H}_{16}$  mixtures at 800 K, and their inhibitory effects first increase and then decrease with increases in the temperature. R231, R243, and R238 also have significant inhibitory effects on the IDTs at 800 K, and the inhibitory effects of R231 and R243 decrease when the temperature increases, whereas the inhibitory effect of R238 increases with increases in the temperature and R238 has the greatest inhibitory effect on the IDTs at 1100 K. The promoting effects of R244 and R178 are the greatest at 800 K, and their promoting effects first increase and then decrease with increases in the temperature. R337 and R170 also have a significant promotional effect on the IDTs at 800 K, and their promoting effects decrease with the temperature increasing. At 800 K, the promoting effect of R239 is small, but it increases with increases in the temperature. Figure 21c shows that the chemical effect has an inhibitory effect on R176 and R178 at 800 K, but has a promoting effect at 900 K and 1100 K. The chemical effect of n-heptane has a promotional effect on the sensitivity coefficients of reactions related to ammonia. Figure 21b depicts that O radical has an inhibitory effect on the sensitivities of reactions associated with n-heptane at 800 K, but has a promoting effect on those at 900 K and 1100 K. The sensitivities of reactions associated with ammonia are enhanced by O radical at all three temperatures.

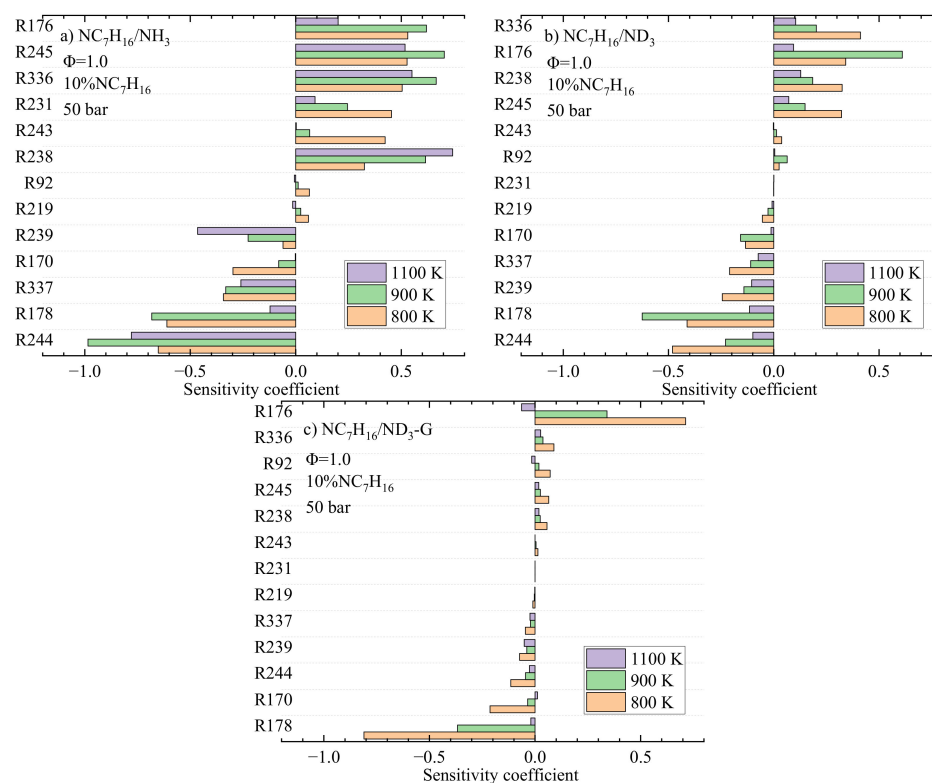


**Figure 21.** Sensitivity of IDTs for  $\text{NH}_3/\text{NC}_7\text{H}_{16}$  mixtures at 800 K, 900 K, and 1100 K,  $\Phi = 1.0$ ,  $p = 50$  bar, and a n-heptane mass fraction of 10%, (a)  $\text{NH}_3/\text{NC}_7\text{H}_{16}$ , (b)  $\text{ND}_3/\text{NC}_7\text{H}_{16}$ , and (c)  $\text{ND}_3/\text{NC}_7\text{H}_{16}\text{-G}$ .

Figure 22a,c shows that, at  $\Phi = 1.0$ , the impact of the chemical effect on the sensitivity coefficients is similar to that at an equivalence ratio of 0.5. Figure 22b,c depicts that O radical has an inhibitory effect on the sensitivities of reactions associated with n-heptane at 800 K, but has a promoting effect on those at 900 K and 1100 K. Under the thermal effect + the effect of O radical or only the thermal effect, only reactions related to n-heptane have a significant effect on the IDTs of  $\text{NH}_3/\text{NC}_7\text{H}_{16}$  mixtures at a n-heptane mass fraction of 30%, whereas reactions related to ammonia have almost no effect on the ignition.

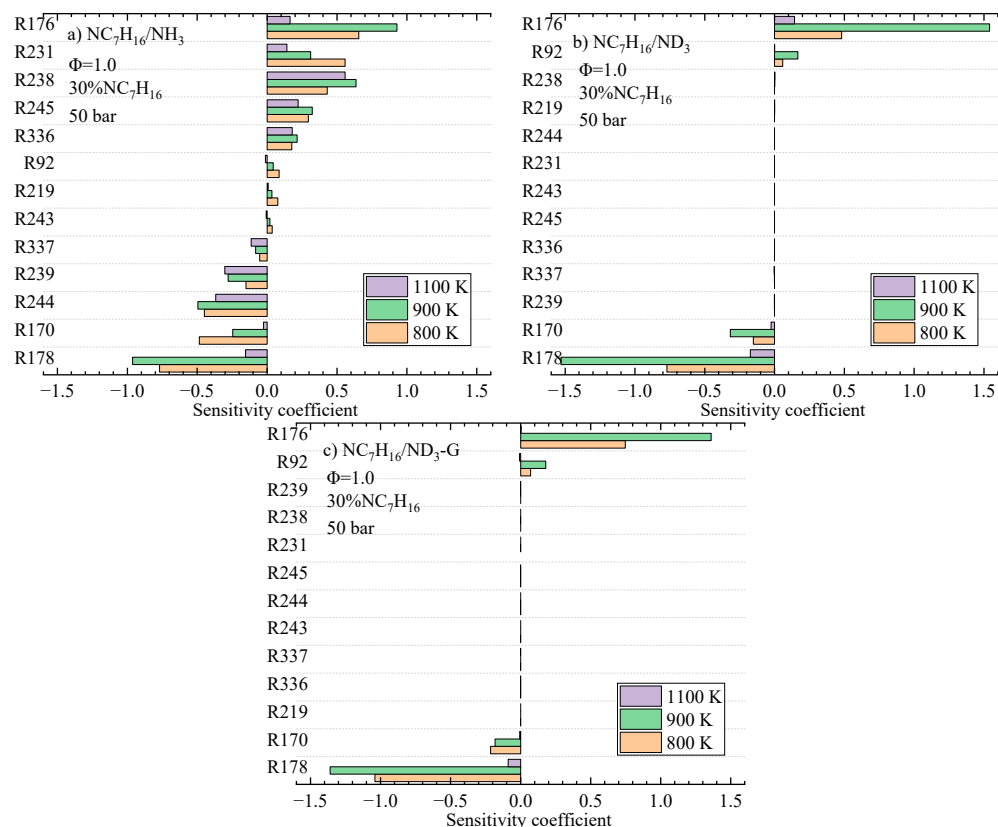


**Figure 22.** Sensitivity of IDTs for  $\text{NH}_3/\text{NC}_7\text{H}_{16}$  mixtures at 800 K, 900 K, and 1100 K,  $\Phi = 1.0$ ,  $p = 50$  bar, and a n-heptane mass fraction of 30%, (a)  $\text{NH}_3/\text{NC}_7\text{H}_{16}$ , (b)  $\text{ND}_3/\text{NC}_7\text{H}_{16}$ , and (c)  $\text{ND}_3/\text{NC}_7\text{H}_{16}\text{-G}$ .

#### 4. Conclusions

In the current study, the chemical effect and the thermal effect of n-heptane on the IDTs of ammonia were investigated. Moreover, an analysis of the time evolution of fuels and a ROP analysis were performed under different effects. Finally, sensitivity analysis was conducted under different effects to further understand the chemical effect and the thermal effect of n-heptane on the IDTs of ammonia. The main conclusions are as follows:

1. The mixing of ammonia has a significant influence on the IDTs of n-heptane, and there was no the NTC behavior that was not observed under all three cases at a n-heptane mass fraction of 10%. As the n-heptane mass fraction increases to 20%, NTC behavior is observed in the IDTs of  $\text{NC}_7\text{H}_{16}/\text{ND}_3$  and  $\text{NC}_7\text{H}_{16}/\text{ND}_3\text{-G}$ . As the n-heptane mass fraction increases to 30%, NTC behavior is observed in the IDTs of all three groups. When the n-heptane mass fraction is 10%, the chemical effect has a significant promoting effect on the IDTs of ammonia/n-heptane mixtures at low and medium temperatures, and the promoting effect is negligible at high temperatures. O radical has a significant promoting effect on the IDTs of ammonia, and the promoting effect decreases with increases in the temperature;
2. The consumption of n-heptane happens prior to that of ammonia, and the rapid consumption of ammonia happens near the ignition timing for all three cases. At 800 K, the time evolution of n-heptane for  $\text{NC}_7\text{H}_{16}/\text{ND}_3\text{-G}$  can be divided into three stages: (a) almost no consumption stage, (b) rapid consumption stage, and (c) slow consumption stage. The chemical effect has an inhibitory effect on the rapid consumption stage, while O radical has a promoting effect on the rapid consumption stage. The rapid consumption stage is mitigated by the increases in temperature. The early increase in temperature is mainly contributed by the oxidation of n-heptane, while

- the increase in temperature during the ignition processes of ammonia/n-heptane mixtures is mainly contributed by the oxidation of ammonia;
3. The chemical effect has no significant promoting or inhibitory effect on R10|G10 and R12|G12, but has an inhibitory effect on R230 and R249. The chemical effect can advance the maximum values of the ROPs of O radical to a lower temperature, and this advancing effect increases with increases in the n-heptane mass fraction. O radical can also advance the maximum reaction rates of the ROPs of O radical to a lower temperature, but it will lead to a decrease in the maximum values of ROPs at a n-heptane mass fraction of 10%. As the n-heptane mass fraction increases, O radical still has a significant effect on the maximum reaction rates of R10|G10 and R12|G12, but has a promoting effect on the maximum reaction rates of R230 and R249;
  4. The chemical effect has a promoting effect on the sensitivity coefficients of all 13 reactions at a n-heptane mass fraction of 10%. When the n-heptane mass fraction is 30%, the chemical effect still has a promotional effect on the sensitivity coefficients of reactions related to ammonia, but has an inhibitory effect on the sensitivities of reactions associated with n-heptane at 800 K and 900 K. O radical has a promoting effect on the sensitivities of reactions associated with ammonia. O radical has an inhibitory effect on the sensitivities of reactions associated with n-heptane at 800 K and 1100 K, but has a promoting effect on those at 900 K. When the n-heptane mass fraction is 30%, the chemical effect has an inhibitory effect on the sensitivities of reactions associated with n-heptane at 800 K and 900 K, but has a promoting effect on those at 1100 K. The chemical effect has a promoting effect on the sensitivities of reactions associated with ammonia at all three temperatures. O radical has a slight inhibitory effect on the sensitivities of reactions associated with n-heptane at 800 K and 900 K, but has a promoting effect on those at 1100 K. Moreover, O radical has a slight promotional effect on the sensitivity coefficients of reactions related to ammonia.

**Author Contributions:** Writing—Original draft, Z.L.; Investigation, Z.L.; Software, Z.L.; Data curation, Y.Z.; Validation, Y.Z.; Formal analysis, Y.Z.; Resources, J.L. and H.W.; Supervision, J.L., C.X. and H.L.; Writing—review and editing, J.L.; Funding acquisition, J.S., H.J., H.L., X.W. and H.Z. All authors have read and agreed to the published version of the manuscript.

**Funding:** This research was funded by Key Research and Development Projects of Ministry of Science and Technology of People’s Republic of China (2023YFE0115300), Industrial and Information Industry Transformation and Upgrading Special Project of Jiangsu Province and Major Science and Technology Project of Zhenjiang.

**Data Availability Statement:** The data presented in this study are available on request from the corresponding author.

**Conflicts of Interest:** Authors Jingrui Li, Changchun Xu, Jianhua Shen and Haiguo Jing were employed by the company CSSC Marine Power Zhenjiang Co., Ltd. Other authors declare no conflicts of interest.

## Nomenclature

IDT	Ignition delay time
NTC	Negative temperature coefficient
ROP	Rate of consumption and production
RCM	Rapid compression machine
ST	Shock tube

## References

1. Reitz, R.D. Directions in internal combustion engine research. *Combust. Flame* **2013**, *160*, 1–8. [[CrossRef](#)]
2. Menegaki, A.N.; Tsarakakis, K.P. Rich enough to go renewable, but too early to leave fossil energy? *Renew. Sustain. Energy Rev.* **2015**, *41*, 1465–1477. [[CrossRef](#)]
3. Shafiee, S.; Topal, E. When will fossil fuel reserves be diminished? *Energy Policy* **2009**, *37*, 181–189. [[CrossRef](#)]

4. Foxon, T.J. A coevolutionary framework for analysing a transition to a sustainable low carbon economy. *Ecol. Econ.* **2011**, *70*, 2258–2267. [[CrossRef](#)]
5. Chu, H.; Ya, Y.; Nie, X.; Qiao, F.; Jiaqiang, E. Effects of adding cyclohexane, n-hexane, ethanol, and 2,5-dimethylfuran to fuel on soot formation in laminar coflow n-heptane/iso-octane diffusion flame. *Combust. Flame* **2021**, *225*, 120–135. [[CrossRef](#)]
6. Liu, L.; Wu, Y.; Wang, Y. Numerical investigation on the combustion and emission characteristics of ammonia in a low-speed two-stroke marine engine. *Fuel* **2022**, *314*, 122727. [[CrossRef](#)]
7. Dimitriou, P.; Javaid, R. A review of ammonia as a compression ignition engine fuel. *Int. J. Hydrogen Energy* **2020**, *45*, 7098–7118. [[CrossRef](#)]
8. Kim, K.; Roh, G.; Kim, W.; Chun, K. A Preliminary Study on an Alternative Ship Propulsion System Fueled by Ammonia: Environmental and Economic Assessments. *J. Mar. Sci. Eng.* **2020**, *8*, 183. [[CrossRef](#)]
9. Kobayashi, H.; Hayakawa, A.; Somarathne, K.K.A.; Okafor, E.C. Science and technology of ammonia combustion. *Proc. Combust. Inst.* **2019**, *37*, 109–133. [[CrossRef](#)]
10. Lesmana, H.; Zhang, Z.; Li, X.; Zhu, M.; Xu, W.; Zhang, D. NH<sub>3</sub> as a Transport Fuel in Internal Combustion Engines: A Technical Review. *J. Energy Resour. Technol.* **2019**, *141*, 070703. [[CrossRef](#)]
11. Lhuillier, C.; Brequigny, P.; Contino, F.; Mounaïm-Rousselle, C. Experimental study on ammonia/hydrogen/air combustion in spark ignition engine conditions. *Fuel* **2020**, *269*, 117448. [[CrossRef](#)]
12. Koike, M.; Suzuoki, T.; Takeuchi, T.; Homma, T.; Hariu, S.; Takeuchi, Y. Cold-start performance of an ammonia-fueled spark ignition engine with an on-board fuel reformer. *Int. J. Hydrogen Energy* **2021**, *46*, 25689–25698. [[CrossRef](#)]
13. Haputhanthri, S.O.; Maxwell, T.T.; Fleming, J.; Austin, C. Ammonia and Gasoline Fuel Blends for Spark Ignited Internal Combustion Engines. *J. Energy Resour. Technol.* **2015**, *137*, 062201. [[CrossRef](#)]
14. Frigo, S.; Gentili, R.; Doveri, N. *Ammonia Plus Hydrogen as Fuel in a S.I. Engine: Experimental Results*; SAE Technical Paper, 2012-32-0019; SAE International: Warrendale, PA, USA, 2012.
15. Starkman, E.S.; Newhall, H.K.; Sutton, R.; Maguire, T.; Farbar, L. Ammonia as a Spark Ignition Engine Fuel: Theory and Application. *SAE Trans.* **1966**, *75*, 660150.
16. Lhuillier, C.; Brequigny, P.; Contino, F.; Mounaïm-Rousselle, C. Experimental investigation on ammonia combustion behavior in a spark-ignition engine by means of laminar and turbulent expanding flames. *Proc. Combust. Inst.* **2021**, *38*, 5859–5868. [[CrossRef](#)]
17. Lhuillier, C.; Brequigny, P.; Contino, F.; Rousselle, C. *Performance and Emissions of an Ammonia-Fueled SI Engine with Hydrogen Enrichment*; SAE Technical Paper, 2019-24-0137; SAE International: Warrendale, PA, USA, 2019.
18. Starkman, E.S.; James, G.E.; Newhall, H.K. Ammonia as a Diesel Engine Fuel: Theory and Application. *SAE Trans.* **1967**, *76*, 670946.
19. Reiter, A.J.; Kong, S.-C. Diesel Engine Operation Using Ammonia as a Carbon-Free Fuel. In Proceedings of the ASME 2010 Internal Combustion Engine Division Fall Technical Conference, San Antonio, TX, USA, 12–15 September 2010; pp. 111–117.
20. Reiter, A.J.; Kong, S.-C. Combustion and emissions characteristics of compression-ignition engine using dual ammonia-diesel fuel. *Fuel* **2011**, *90*, 87–97. [[CrossRef](#)]
21. Niki, Y.; Nitta, Y.; Sekiguchi, H.; Hirata, K. Diesel Fuel Multiple Injection Effects on Emission Characteristics of Diesel Engine Mixed Ammonia Gas into Intake Air. *J. Eng. Gas Turbines Power* **2019**, *141*, 061020. [[CrossRef](#)]
22. Feng, Y.; Zhu, J.; Mao, Y.; Raza, M.; Qian, Y.; Yu, L.; Lu, X. Low-temperature auto-ignition characteristics of NH<sub>3</sub>/diesel binary fuel: Ignition delay time measurement and kinetic analysis. *Fuel* **2020**, *281*, 118761. [[CrossRef](#)]
23. Neely, G.D.; Florea, R.; Miwa, J.; Abidin, Z. *Efficiency and Emissions Characteristics of Partially Premixed Dual-Fuel Combustion by Co-Direct Injection of NG and Diesel Fuel (DI2)—Part 2*; SAE Technical Paper 2017-01-0766; SAE International: Warrendale, PA, USA, 2017.
24. Curran, H.; Gaffuri, P.; Pitz, W.; Westbrook, C. A Comprehensive Modeling Study of n-Heptane Oxidation. *Combust. Flame* **1998**, *114*, 149–177. [[CrossRef](#)]
25. Zhang, K.; Banyon, C.; Bugler, J.; Curran, H.J.; Rodriguez, A.; Herbinet, O.; Battin-Leclerc, F.; B'Chir, C.; Heufer, K.A. An updated experimental and kinetic modeling study of n-heptane oxidation. *Combust. Flame* **2016**, *172*, 116–135. [[CrossRef](#)]
26. Yu, L.; Zhou, W.; Feng, Y.; Wang, W.; Zhu, J.; Qian, Y.; Lu, X. The effect of ammonia addition on the low-temperature autoignition of n-heptane: An experimental and modeling study. *Combust. Flame* **2020**, *217*, 4–11. [[CrossRef](#)]
27. Dong, S.; Wang, B.; Jiang, Z.; Li, Y.; Gao, W.; Wang, Z.; Cheng, X.; Curran, H.J. An experimental and kinetic modeling study of ammonia/n-heptane blends. *Combust. Flame* **2022**, *246*, 112428. [[CrossRef](#)]
28. Zhang, Y.; Zhou, W.; Liang, Y.; Yu, L.; Lu, X. An experimental and detailed kinetic modeling study of the auto-ignition of NH<sub>3</sub>/diesel mixtures: Part 1—NH<sub>3</sub> substitution ratio from 20% to 90%. *Combust. Flame* **2023**, *251*, 112391. [[CrossRef](#)]
29. Zhang, Y.; Liang, Y.; Zhou, W.; Yu, L.; Lu, X. An experimental and detailed kinetic modeling study of the auto-ignition of NH<sub>3</sub>/diesel mixtures: Part 2—Wide pressures up to 120 bar. *Combust. Flame* **2024**, *259*, 113131. [[CrossRef](#)]
30. Wen, M.; Liu, H.; Cui, Y.; Ming, Z.; Feng, L.; Wang, G.; Yao, M. Study on combustion stability and flame development of ammonia/n-heptane dual fuel using multiple optical diagnostics and chemical kinetic analyses. *J. Clean. Prod.* **2023**, *428*, 139412. [[CrossRef](#)]
31. Thorsen, L.S.; Jensen, M.S.; Pullich, M.S.; Christensen, J.M.; Hashemi, H.; Glarborg, P.; Alekseev, V.A.; Nilsson, E.J.; Wang, Z.; Mei, B.; et al. High pressure oxidation of NH<sub>3</sub>/n-heptane mixtures. *Combust. Flame* **2023**, *254*, 112785. [[CrossRef](#)]

32. Song, M.; Wang, Q.; Wang, Z.; Fang, Y.; Qu, W.; Gong, Z.; Feng, L. Auto-ignition characteristics and chemical reaction mechanism of ammonia/n-heptane mixtures with low n-heptane content. *Fuel* **2024**, *364*, 131011. [[CrossRef](#)]
33. Huang, Z.; Wang, H.; Luo, K.; Fan, J. Direct numerical simulation of ammonia/n-heptane dual-fuel combustion under high pressure conditions. *Fuel* **2024**, *367*, 131460. [[CrossRef](#)]
34. Li, J.; Huang, H.; Kobayashi, N.; Wang, C.; Yuan, H. Numerical study on laminar burning velocity and ignition delay time of ammonia flame with hydrogen addition. *Energy* **2017**, *126*, 796–809. [[CrossRef](#)]
35. Sun, W.; Lin, S.; Zhang, H.; Guo, L.; Zeng, W.; Zhu, G.; Jiang, M. A reduced combustion mechanism of ammonia/diesel optimized with multi-objective genetic algorithm. *Def. Technol.* **2024**, *34*, 187–200. [[CrossRef](#)]
36. Wang, B.; Dong, S.; Jiang, Z.; Gao, W.; Wang, Z.; Li, J.; Yang, C.; Wang, Z.; Cheng, X. Development of a reduced chemical mechanism for ammonia/n-heptane blends. *Fuel* **2023**, *338*, 127358. [[CrossRef](#)]
37. Mathieu, O.; Petersen, E.L. Experimental and modeling study on the high-temperature oxidation of Ammonia and related NOx chemistry. *Combust. Flame* **2015**, *162*, 554–570. [[CrossRef](#)]

**Disclaimer/Publisher’s Note:** The statements, opinions and data contained in all publications are solely those of the individual author(s) and contributor(s) and not of MDPI and/or the editor(s). MDPI and/or the editor(s) disclaim responsibility for any injury to people or property resulting from any ideas, methods, instructions or products referred to in the content.